MARITIME SOLUTIONS FOR A CHANGING WORLD

#167 - AUTUMN 2022

TERRA ET AQUA

ESTIMATING SEDIMENT EROSION

Research paper by Suman Sapkota, winner of IADC's Young Author Award

CLIMATE RISK OVERVIEW TOOL

Mapping nature-based flood protection opportunities

IADC SAFETY AWARDS 2022

ENCOURAGING THE DEVELOPMENT OF SAFETY

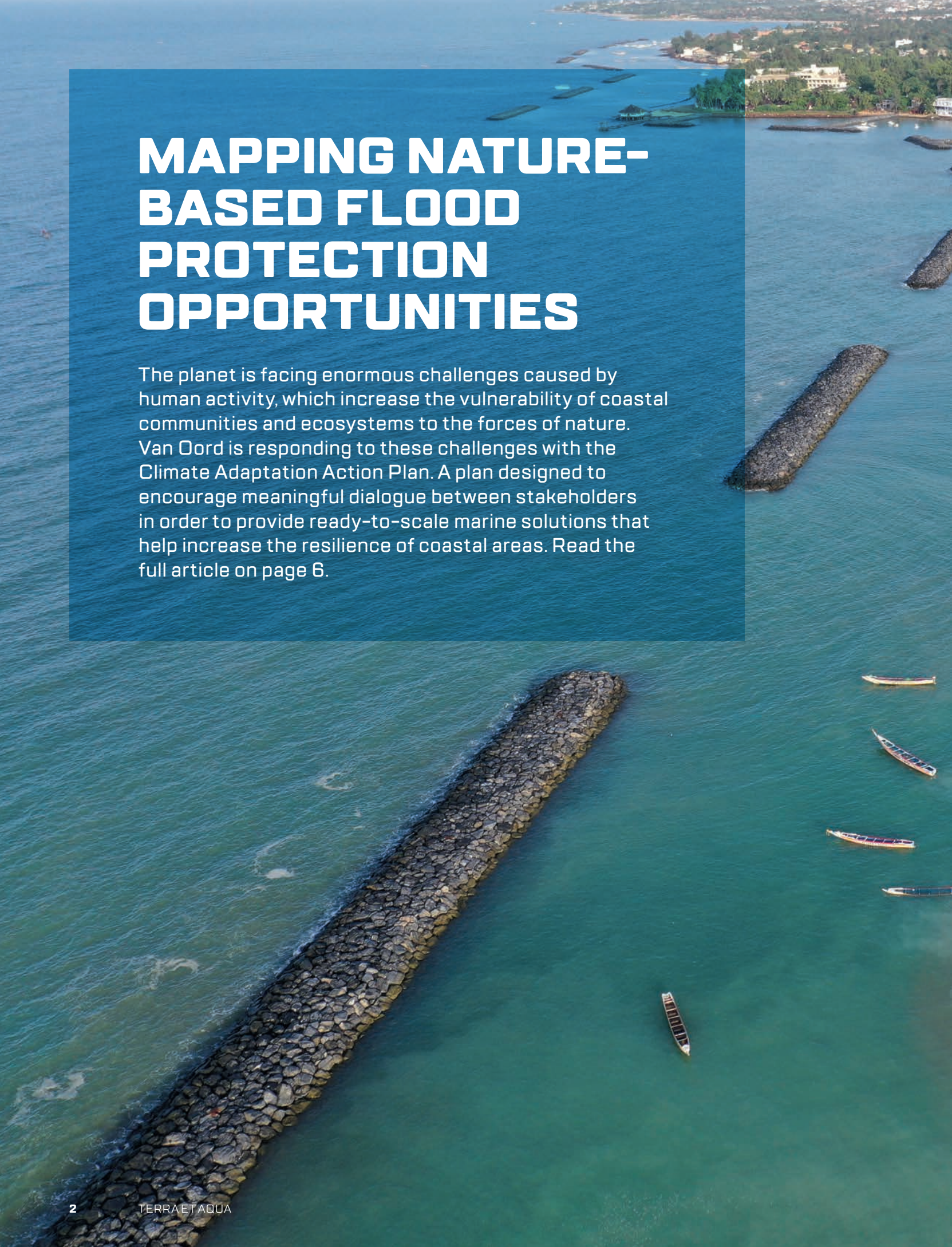

MAPPING NATURE-BASED FLOOD PROTECTION OPPORTUNITIES

The planet is facing enormous challenges caused by human activity, which increase the vulnerability of coastal communities and ecosystems to the forces of nature. Van Oord is responding to these challenges with the Climate Adaptation Action Plan. A plan designed to encourage meaningful dialogue between stakeholders in order to provide ready-to-scale marine solutions that help increase the resilience of coastal areas. Read the full article on page 6.

CONTENTS

CONTRIBUTING TO A NET-ZERO WORLD

One thing that is certain is it's going to take collaboration to tackle climate change and to reach the goals set by the Paris Agreement.

The global move from fossil fuels to renewables is top of the agenda for industry. The goal to reach the 2050 decarbonisation target set by the 2015 Paris Agreement is clear. For the dredging sector, that means moving away from the classical energy drivers of trenching and backfilling in the building of gas terminals, for example, and moving towards new interpretations of that driver with seabed preparations and scour protection of offshore wind farms.

One of the heralded solutions in the maritime industry is the use of LNG vessels. Ships are now equipped with dual fuel although LNG equipment requires additional investment. CIRIA has recently published three sustainability factors developed for this purpose. Other fuels, such as ammonia, methanol and hydrogen are also being developed. The first dual fuel methanol vessel has been ordered and will be delivered in 2024.

The availability of new fuels however, is still uncertain and may act as a brake on the energy transition. While renewables are already often cheaper than fossil fuel power in much of the world, the crisis in the Ukraine has seen prices of LNG increase. More costs means projects become more expensive, which could also serve to slow the transition to a net-zero world.

Conducting joint research to be able to work more sustainably makes the dredging sector stronger and reduces risks in undertaking these studies. In addition, working together on a level playing field in the application of sustainability criteria in tenders also increases the social value of individual projects and thus of our sector. The sharing of information is therefore key.

A prime example is the Climate Risk Overview tool. Developed by Van Oord, this web-based global mapping tool brings together key parameters, such as populations, low-lying land and expected sea level rise to anticipate the hazard of flooding for all coastlines and societies around the world. Free to use, the tool and its information is available for everyone to explore and provides a useful resource for potential climate adaptation projects across the globe. You can read the full article on page 6.

Other articles in this issue include a roundup of all the submissions in the running for IADC's Safety Awards 2022, along with the winning technical article from the recipient of this year's Young Author Award, presented to Suman Sapkota at WODCON XXIII in Copenhagen in May.

Frank Verhoeven
President, IADC

> **Conducting joint research to be able to work more sustainably makes the dredging sector stronger.**

Saly, Senegal

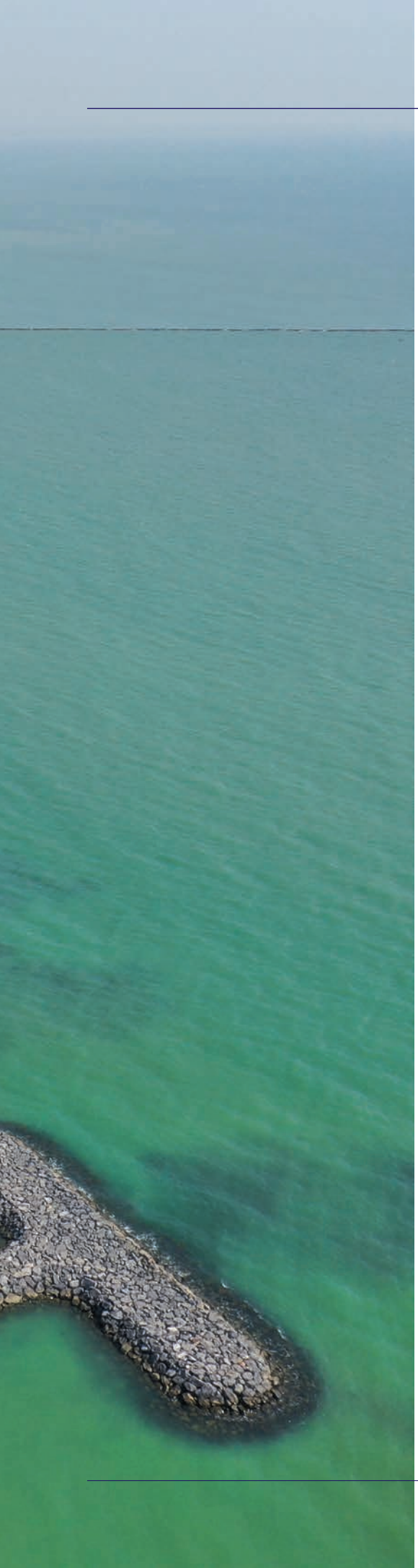

CLIMATE RISK OVERVIEW TOOL: MAPPING NATURE-BASED FLOOD PROTECTION OPPORTUNITIES

The planet is facing enormous challenges caused by human activity, increasing the vulnerability of communities and ecosystems to the forces of nature. This is worsened by the effects of climate change, which is threatening the world's coastal defences. Van Oord has responded to these challenges by developing the Climate Adaptation Action Plan. The plan is designed to encourage meaningful dialogue between stakeholders in order to provide ready-to-scale marine solutions that help increase the resilience of the communities and ecosystems of coastal areas.

In 2018, Van Oord marked its 150th anniversary with an international symposium with climate change and the energy transition as major themes. Invited to speak at the symposium was Christiana Figueres, the United Nations' top climate change diplomat who delivered the Paris Agreement in 2015. She gave a powerful speech on the importance of achieving the climate agreements to combat global warming. She emphasised the need for action from both state and non-state actors to limit the effects of climate change, particularly for the world's most vulnerable coastal communities.

Van Oord responded to this call for action by developing the Climate Adaptation Action Plan, designed to encourage dialogue between stakeholders and provide ready-to-scale marine solutions that help increase the resilience of coastal areas, their communities and ecosystems. Our sustainability programme, S.E.A. (Sustainable Earth Actions), focuses on four pillars:

- Enhancing the energy transition
- Accelerating climate action
- Empowering nature and communities
- Achieving net-zero emissions by 2050

The Climate Adaptation Action plan is one of the initiatives under the pillar 'accelerating climate action'. We believe that collaboration with all stakeholders on climate actions is needed to be able to make a greater positive impact.

The pillar 'empowering nature and communities' impacts our day-to-day actions for 'accelerating climate action'. For example, making use of mangrove rehabilitation for flood protection while empowering local communities to create new opportunities for economic benefits and social impact. The involvement of local communities is pivotal in making our marine and Nature-based Solutions (NbS) as effective and sustainable as possible. Our experience and expertise in ocean health, such as restoring marine ecosystems like coral, oyster beds and seagrasses, only developed through the extensive collaboration with local communities and world-renowned research institutions around the globe. The pillar 'achieving net-zero emissions by 2050' also affects which opportunities we invest in for 'accelerating climate action'. On the one hand, we advocate solutions that have a smaller CO2 footprint, for instance by choosing natural materials like sand over concrete and by choosing designs that require smaller equipment and hence less fuel. On the other hand, we advocate solutions that can act as a carbon sink, for instance mangroves are an important opportunity for carbon sequestration (Chatting et al, 2022).

This year, the world's largest humanitarian network, the International Federation of Red Cross and Red Crescent Societies (IFRC) and one of the world's largest and most experienced conservation organisations, the World Wildlife Fund for Nature (WWF) released a report with a call to action (IFRC and WWF, 2022). It urges the private sector to: 'Scale up investment in existing forms of private sector finance mechanisms for NbS. Invest in exploring innovative new finance mechanisms (such as insurance mechanisms) for NbS for climate adaptation and disaster risk reduction, establishing their scale-up potential and feasibility in different geographies.' It advocates a fast track process led by the private sector, in addition to the regular government-led tender-process. Van Oord wants to take the lead in taking action in the private sector of the maritime engineering industry and is dedicated to being a proactive partner in this quest. The launch of our Climate Adaptation Action Plan is a pro-active early stage process that will complement the regular business development process with new projects by exploring new finance mechanisms for delivering our established solutions together with the right partners.

The Climate Adaptation Action Plan consist of three elements (Figure 1). The first stage is to make a **Climate Risk Overview** (CRO). Basically an advanced geospatial multi-criteria analysis, the CRO is a global tool where open source data is mapped onto 10 km segments of the world's coastlines. The overview brings together key parameters, such as populations, low-lying land and expected sea level rise to anticipate the hazard of flooding for all coastlines and societies around the world. Deploying this tool allows us to start and support dialogues with various stakeholders and to focus our efforts on potential climate adaptation projects. Designed to be a fast and intuitive tool for quick selection, the CRO and its information is available for everyone to explore. In contrast to a heuristic bottom-up approach where locations are added to a selection until the selection is large enough for a portfolio of locations, the CRO offers a systematic global top-down approach where locations are dropped until a small enough portfolio of locations is left. For this workflow, the CRO uses readily available global data sources. These sources are often based on satellite data that have some methodical and sensor limitations. Therefore, the numbers shown in the tool are not to be used at face value, but in a relative sense to compare locations. Each selection of a location needs further verification using detailed data sets. The CRO is meant to be used in a cycle back and forth with detailed GIS software. The result is a shortlist of approximately ten potential locations where a climate adaptation project could be initiated. These will subsequently be analysed in the context of the natural and societal systems.

The second element of the Climate Adaptation Action Plan is **Climate Adaptation Solutions**. Using the short list of potential locations created from the CRO, each location is then studied in detail. A system analysis as proposed by the Building with Nature concept (de Vriend et al, 2015) is executed to facilitate maximal synergy with the ecological context. The available Building with Nature solutions, for example permeable dams (Winterwerp et al., 2020) are mapped against the local challenges to select viable solution strategies. This stage requires detailed analyses in dedicated GIS software using a combination of global and local data. This will result in suitable ranges of solutions for each location. Some locations might not be viable and will be dropped at this stage. If too few locations remain, the CRO step will be repeated.

The third step is the **Climate Adaptation Action Coalitions**. After investigating each location with its natural context, each location is analysed in terms of the societal system in which it is located. Just as Building with Nature, this will also be carried out with a range of partners. For this purpose, Van Oord has become an active member of various international groups, alliances and networks, notably Ocean Risk and Resilience Action Alliance (ORRAA). This stage requires detailed societal analyses in using a combination of global and local networks. A site visit to meet local partners is crucial. In addition, after this stage some locations might be found less suitable to pursue for a variety of reasons.

After these three steps of the Climate Adaptation Action Plan are completed, a handful of locations are classified as suitable for further development. At this stage, these potential locations are jointly developed with the commercial department within the dredging business unit of Van Oord as a new project lead that requires follow-up. The three steps of the Climate Adaptation Action Plan will be repeated from time to time to ensure that we continuously investigate and identify potential locations that can be protected from the consequences of climate change. Van Oord is currently in the process of finishing a first iteration cycle. When the next cycle starts, we anticipate adding new data layers to the CRO to detect new business opportunities around the world that were not yet visible.

Climate Risk Overview

The Climate Risk Overview tool has been described by de Boer et al. (2022). Their paper described the basic elements in detail: the systematic global screening grid and the calculation of the number of people exposed to flooding. These aspects are summarised below. Four additional layers

FIGURE 1

The 3 steps of Climate Adaptation Action Plan that are necessary to supply potential projects to our business development.

of the CRO, which were not described by de Boer et al. (2022), will be introduced here: the community aspect via World Bank income level and resilience, and the ecosystem aspect via mangroves and corals.

The site selection and exposure to flooding

For the purpose of screening the entire planet for a combination of parameters, we start our search with the area that is at risk. This is the global Low Elevation Coastal Zone (LECZ), defined as the part of the land that is lower than 10 metres above mean sea level. We used a Digital Elevation Model (DEM) to calculate the global contour of the land 10 metres above sea level. At the sea side, we take the -50 metres depth contour to encompass all marine locations that may act as a source of sediment and could accommodate land reclamations. We used a space filling algorithm to divide the strip of land between these contours into sites of approximately 10 x 10 km² = 100 km². The world's coastline was then used to split each site into wet and dry areas. For the current analyses, we kept only those sites that are at least partially covered with land. The remaining sites are irregularly shaped. The typical size of 100 km² was chosen because it is an upper size at which communities can be informally addressed. It is also the spatial scale of local habitats, which is the typical scale at which geomorphological solutions evolve. This yielded 60,000+ sites worldwide.

The essence of the idea behind Climate Risk Overview is to combine data from a range of different sources from different disciplines for each site. We programmed a range of python modules for different data types. First, detailed grid data needs to be averaged to the sites. This is the case for global digital elevation models with a resolution of 30 m (SRTMv4, NASADEM, ALOS, MERIT), and for population data that is available at 100 m resolution (GPWv4, WorldPop). Second, coarse gridded data needs to be interpolated. Examples of this are the IPCC sea level rise projections. Third, vector data needs GIS software to calculate the overlap area. This is the case for mangrove and coral coverage patches. Also, country data is treated as vector data. Lastly, for point data sources we assigned each object to the nearest site, with a maximum distance. This is the case for the global tide and storm data sets.

Boer et al. (2022) calculated the Extreme Sea Level (ESL) for different scenarios per hotspot and combined that with the local DEM and population data to calculate the population exposed to flood risk for each site. The 2090 scenario with 1/100 year flood exposure was added to the public CRO. With this layer, sites that are prone to flooding can be detected. With the additional layers below, it is possible to filter the sites for the ecological purpose of Climate Adaptation Solutions and for the societal purpose of the Climate Adaptation Coalitions.

Communities: resilience and income level

In order to find those communities that need sustainable climate adaption solutions, we needed a compound measure to detect those sites. The most appropriate measure is the Notre Dame Global Adaptation Initiative (ND-GAIN) index (Chen et al, 2015). It is a compound measure that combines the

vulnerability to climate change of a country with its readiness to improve. These two measures are based on respectively 36 detailed and 9 base indicators. The resilience is the readiness minus the vulnerability. The resulting normalised ND-GAIN is a number between 0 and 100, with a higher value being better. Most European countries have values in the range of 60-80, whereas developing countries in Africa have values in the range of 20-30.

A second measure we show in the CRO is the World Bank income level. The World Bank assigns the world's economies to four income groups: low, lower-middle, upper-middle and high-income countries. The split is based on the Gross National Income (GNI) per capita.

Unfortunately, the underlying ND-GAIN indicators are country aggregates, so the ND-GAIN has only one value per country. The same is valid for World Bank data. For large countries, this leads to inherent lack of spatial drill-down resolution in site selection in the CRO. Despite this drawback, this is the best measure available for this purpose.

% Coverage (rounded)	# Number of CRO sites	Mangrove km²
0	54,365	2,892
10	2,814	8,888
20	1,441	9,272
30	990	9,306
40	712	9,372
50	499	9,062
60	347	7,310
70	241	8,462
80	124	4,953
90	43	1,651
100	13	5
Grand Total	**61,589**	**71,172**

TABLE 1

Mangrove distribution over the sites per 10% area coverage.

Ecosystems: mangroves

Using the resilience and the income level, it is possible to detect the areas that would benefit most from proactive climate adaptation projects. These are concentrated and located in semi-tropical climates. The most promising coastal ecosystems for climate adaptation solution in those areas are mangroves and corals. For this reason, we prioritised the addition of those two ecosystems to the CRO. We plan to add data from other ecosystems in the future, such as seagrasses and salt marshes. We chose to use the data from Global Mangrove Watch (GMW) (Bunting et al., 2018). GMW has global mangrove cover for 7 years between 1996 and 2016. The data is based on satellite data and has a resolution of 30 m. This data set allows detecting changes in mangroves and classifying each pixel as maintained, lost or gained. To avoid complexity in the early search stage for which our CRO is meant, we chose to process mangrove data for the latest year, 2016. The presence of mangroves shows climatological suitability for mangrove restoration. It is also a base for prevention projects, as the current mangrove deforestation rates are 3.5-8% in Asia (Hamilton and Casey, 2020).

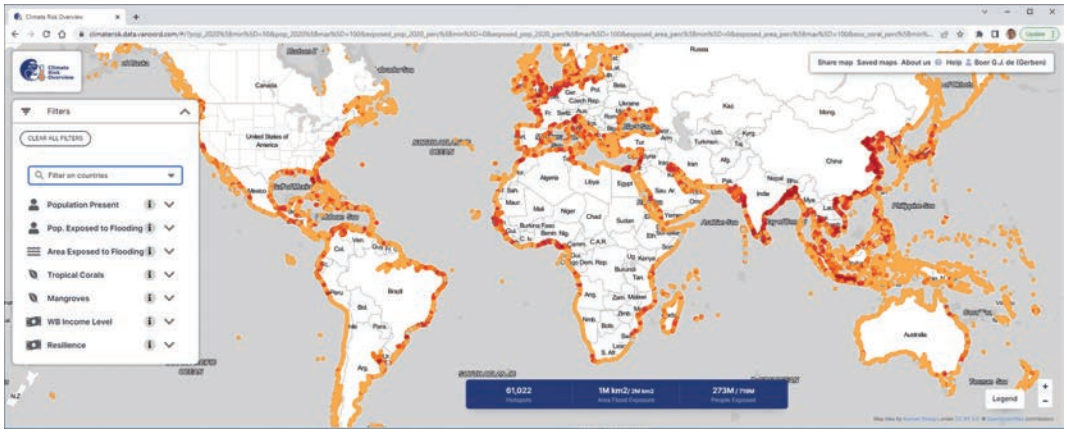

A

B

C

D

FIGURE 2A-D

The Climate Risk Overview https://climaterisk.data.vanoord.com: (A) 61,022 hotspots from which (B) 27,283 hotspots have <50% resilience, (C) hotspots that also have 20% mangrove coverage and (D) 929 hotspots that also have at least 50% of the population exposed to flood risk.

Per site, we calculate the area (km²) of mangroves present and the percentage of the site area that they cover. Table 1 shows that the CRO has 12,324 sites worldwide with mangroves present in them, covering in total 71,172 km². This total number is a little lower than the global area of mangroves as reported by the GMW data processor of 77,000 km² (Bunting et al., 2018). However, a later reprocessing by Hamilton and Casey (2016) shows that the total area of GMW is 69,000 km² for 2014 when using a different definition based on the percentage coverage. We also used percentage coverage in our calculation, so our estimate is close to literature.

Tropical corals

The global tropical corals data set of UNEP et al. (2001) was processed similar to mangroves. The vector data set was used to calculate the area and overlap with our site definitions. Because our site definition includes the underwater foreshore, the CRO does not contain all the world's corals, but only those corals that are in a site that is at least partially covered with land. These are corals that can directly provide ecosystem services to the adjacent areas. This is 6,490 km² of corals of the total world coverage of 284,300 km² (Spalding et al, 2001).

Application

To illustrate the way of working, Figure 2 shows an example drill-down. Selecting a resilience of less than 50% to identify communities that might need assistance, yields 27,283 sites. Also selecting at least 20% mangrove coverage yields 2,975 hotspots. This provides the combined ecological and societal criteria. Finally, we select at least 50% of the population exposed to flood risk, yielding less than 1,000 sites. This number can be further reduced by setting stricter filters, adding other filters or taking other information into account.

Within Van Oord, we have a fully functional extended version of the CRO implemented in our standard business intelligence tool (Qlik Sense). This version differs in three fundamental aspects. Firstly, it is not nearly as polished, user-friendly and fast as the public CRO. Secondly, it is relatively easy to add extra layers because it hardly requires computer programming skills to add new data. This allows us to use the Qlik Sense version as a research and development environment for developing new layers. And thirdly, the data layers in the prototype have not yet passed thorough quality checks and a verification with scientific literature. However, this version does allow us to drill-down further with these draft layers, taking the uncertainties into account. We plan to pass these layers one by one through a quality assurance check and add them to the public CRO. The speed and order of this will be subject to our progress with the Climate Adaptation Action Plan. After each

FIGURE 3

Bacton to Walcott sandscaping (Sand Engine), UK.

FIGURE 4

Hondsbossche and Pettemer sea defence, the Netherlands.

full cycle of the three elements of this plan, a renewed investment effort is made into the public CRO.

Climate Adaptation Solutions

Van Oord has been creating coastal defences across the globe for many years and we are always looking at how we can improve the design and execution of projects. In recent years, we have been more focused on Building with Nature solutions and reducing the impact on the environment. We also see a need from our clients in this direction. Furthermore, it is appreciated when the contractor can bring in their experience and can assist with the design to develop climate adaptation projects in a more environmentally friendly way.

Nature has many ways to defend our coastlines. We can learn from this and are convinced that nature-based solutions will help in tackling societal challenges. When the forces of nature are utilised, opportunities for nature development are strengthened. In turn, more sustainable solutions can be created, adding value to the surrounding area.

The coastal protection solutions can be made from hard elements (grey) or soft elements (green) or a combination of hard and soft elements. Hard structures like revetments, groynes and breakwaters are usually made from rock or concrete precast elements. Sometimes wood is used for groynes. These solutions have the advantage that there are many existing calculating methods to design these works.

The solutions based on soft elements are beach nourishments, dunes, Sand Engines, salt marshes, mangroves and submerged reefs. The advantage of these solutions is that they better fit in the natural environment as natural elements present in the surrounding are used.

The following three examples of coastal protection projects we executed to create value for the environment, economy and society.

To protect the eroding coastline from Bacton to Walcott in the UK (Figure 3), Van Oord created a Sand Engine. To mitigate the eroding coastline threatening infrastructure. The client organised funding from the private and public sector to reinforce the coastline using a new nature-based solution called the Sand Engine (Johnson et al, 2020). The Sand Engine (also called Sand Motor) is a type of beach nourishment where a large volume of sand is added to the coast. The natural forces of wind, waves and tides then distribute the sand along the coast over many years, preventing the need for repetitive beach nourishment.

A great example is the Hondsbossche and Pettemer Zeewering (HPZ) sea defence (Figure 4). Van Oord converted an old hard defence into a soft dune landscape that created more value for the environment and society. The existing dyke was no longer sufficient for future protection. It could not be raised any further within the footprint and therefore the client was open to a novel approach. By using the Building with Nature approach, the level of protection was upgraded with a dune and beach landscape. At the same time, this landscape created a much higher value on nature and recreation purposes (Ecoshape, 2022; Karaliūtė, 2022).

FIGURE 5

Saly, Senegal.

Another example is Saly in Senegal (Figure 5), where the beach had disappeared completely. Houses had been taken by the sea and the tourism industry had completely collapsed. We created a coastal defence over 4 kilometres by protecting the coastline with offshore breakwaters and a beach restoration. As a result, the local fishers now have access to the sea and can store their boats safely in protected calm areas created by the breakwaters. The local economy has recovered as beach tourism started to flourish again.

Climate Adaptation Action Coalitions

Van Oord recognises that the challenges faced and the solutions needed cannot be addressed by us alone. For that reason, we are building a continuously growing network of stakeholders, knowledge institutes, finance institutes and political decision makers. In 2021, Van Oord joined forces with the Ocean Risk and Resilience Action Alliance (ORRAA) and the Global Center on Adaptation (GCA). We also recognise the need to share our solutions and build international networks through participation in events, such as COP26 (UNFCCC Climate Conference) and the UN Ocean Conference.

The global climate crisis can only be solved by collaboration and knowledge sharing, therefore we look to collaborate with various parties from the public and private sector. With everyone working together, all with the same mission, we can accelerate opportunities for scaling up existing and developing new nature-based solutions across the globe to accelerate positive impact for climate adaptation.

To improve on innovative solutions, and ensure longevity and positive impact, collaboration with knowledge institutes like universities and (local) specialists is extremely important. Furthermore, to implement those ideas into designs we need to work together with consultants and clients.

Climate adaption solutions also asks for new financing mechanisms, for different revenues to make the business case and for new structures to bring finance together. For this knowledge and action, input from finance institutes is needed. For example, Carbon Credits and Public-Private-Partnerships (PPP) schemes.

To create added value for the environment, economy and society, it is important to understand the local system and needs from the local stakeholders. A good example

of local coalition forming is our approach in Mozambique (Figure 6) where we are engaging with a broad range of communities trying to understand the local needs and explore long-term sustainable solutions together with them.

Conclusions

With the Climate Risk Overview, Van Oord has created a global mapping tool with many coupled data sources that is proving to be an indispensable tool to assist in a dialogue between multidisciplinary stakeholders. It acts as an easy and immediate fact-based sparring partner to test ideas that arise from an individual idea or from a group session. Equally, we also realise that this web tool cannot capture the whole truth, despite our efforts to make it complete. The use of global data sources provides a fair method to compare sites, but also has disadvantages due to the inherent lack of resolution and/or ground truth. After site selection in the tool to a handful of locations (phase 1), we do a detailed study (phase 2) using local data in a GIS system, and a plethora of map thematic web viewers provided by NGOs, research institutes and others. Noteworthy examples are the Ocean Data Viewer (https://data.unep-wcmc.org) of the UNEP World Conservation Monitoring Centre (UNEP-WCMC) where we downloaded our mangrove and coral data, and mapx (https://www.mapx.org) by UNEP/World Bank that shows population and elevations among others. In these web viewers, individual data layers can be analysed in great detail, but these portals are also silos that do not allow for interaction between the layers.

An intended effect of our decision to make the Climate Risk Overview freely and publicly available is that everyone can and should use it, not just the thematic or policy experts in our field. The Climate Risk Overview proved already to be a tool that is so easy to use that it is a powerful tool for the public to explore. We have used it in sessions with both our clients and with students. We hope it will raise awareness for the great challenges that society faces due to climate change and that it might unlock unexpected opportunities.

Before starting with the Climate Risk Overview, we searched the web for existing global screening initiatives that we could join. We found many wonderful initiatives that share valuable data, but most tended to be for a narrow theme. The ones that could accommodate multidisciplinary data, ranging from population to mangroves, tended to be full-fledged GIS systems beyond the reach of the general public. We experienced that making a global multidisciplinary data analysis tool with many diverse layers is a large effort and we are open to partners who want to collaborate with us on the further development of this tool. The Climate Risk Overview is an essential element in the three-pronged approach to delivering our Climate Adaptation Action Plan.

FIGURE 6

Community meeting (Mozambique).

Summary

This article presents the Climate Adaptation Action Plan developed by Van Oord, which consists of three components. The first is the creation of the Climate Risk Overview (CRO). This is a web-based tool that brings together key parameters, such as populations, low-lying land and expected sea level rise to anticipate the hazard of flooding for all coastlines and societies around the world. It allows anyone to find and assess locations based on the number of people exposed to flooding and the presence of mangroves and corals. The combination of these layers is with the aim to help increase the resilience of the communities and ecosystems of coastal areas. The tool is freely available to allow everyone to use it. Van Oord uses an internal version of the tool in standard business intelligence software to experiment with more layers that, following quality checks, will be used to update the public version. Use of the tool internally allows the company to focus its business development efforts in climate adaptation projects.

The second phase is the process of creating Climate Adaptation Action Solutions. This is an experience record of marine and coastal solutions that we and our partners (for example EcoShape) have delivered in the past. The purpose is to have a ready portfolio of options that can be reused across the globe, with the necessary adaptations to the local social and environmental situation. We use this portfolio to assess sites that pop-up from screening with the CRO. Thirdly, we are forging Climate Adaptation Action Coalitions, a global network of partners with a diverse background, with the purpose of creating multidisciplinary teams suited to make convert climate adaptation from a reactive to a proactive field. This step adds a societal filter to the sites from the CRO.

Gerben J. de Boer

After graduating as a civil engineer, Gerben J. de Boer obtained his doctorate in coastal oceanography from Delft University of Technology (TU Delft) in the Netherlands, focusing on the stratification of the Rhine river plume. He worked for over 10 years at Deltares as a consultant on remote sensing, numerical modelling and data management, and was a member of the MODEG marine data export group to the European Commission. Since 2014, Gerben is the manager of the Datalab at Van Oord's Engineering and Estimating department.

Reinout Viersma

Since graduating from TU Delft in the Netherlands with an MSc, Reinout Viersma has worked in coastal protection, land reclamation, ports & waterway and marine construction. He has worked for Van Oord and predecessors for 25 years in various roles in the execution of dredging and marine construction works, including commercial roles on branch offices around the world and as a tender manager at Van Oord's head office working on large complex projects. Reinout currently works as Programme Manager Climate Adaptation, tasked with developing coastal protection to mitigate climate change.

Rachel Terry

Rachel Terry graduated as a Civil and Coastal Engineer with a masters in engineering (Hons) from the University of Plymouth, in the UK. She combines her technical background with a purpose to contribute to making a better world. Rachel gained design engineer experience on projects in the civil maritime industry and operational experience in offshore wind projects. She is currently the head of Sustainability at Van Oord and strives to support the business to translate its capabilities into creating a net positive impact and a sustainable future.

References

Bunting P., Rosenqvist A., Lucas R., Rebelo L-M., Hilarides L., Thomas N., Hardy A., Itoh T., Shimada M. and Finlayson C.M. (2018)
The Global Mangrove Watch – a New 2010 Global Baseline of Mangrove Extent. *Remote Sensing*, 10(10):1669. DOI:10.3390/rs1010669. Data viewer: https://data.unep-wcmc.org/datasets/45

Chatting M., Al-Maslamani I., Walton M., Skov M.W., Kennedy H.,Sinan Husrevoglu Y. and Le Vay L. (2022)
Frontiers in Marine Science, 10 February. DOI:10.3389/fmars.2022.781876

Chen, C., Noble, I., Hellmann, J., Coffee, J., Murillo, M. and Chawla, N. (2015)
University of Notre Dame Global Adaptation Index. *Country Index Technical Report*. https://gain.nd.edu/our-work/country-index

De Boer G.J., Oudman R.J., Danebjer A.L.C., Jawaid M.Z., Tosun G., Terry R. and Viersma R. (2022)
Climate Risk Overview: Rapid global selection of climate adaptation opportunities. *WODCON XXIII proceedings*, Copenhagen. https://www.dredging.org/resources/ceda-publications-online/conference-proceedings/abstract/1137

De Vriend H.J., van Koningsveld M., Aarninkhof S.G.J., de Vries M.B., Baptist M.J. (2015)
Sustainable hydraulic engineering through building with nature. *Journal of Hydro-environment Research*, 9 (2), 159–171. DOI:10.1016/j.jher.2014.06.004

Ecoshape (2022)
Hondsbossche Dunes. https://www.ecoshape.org/en/pilots/hondsbossche-and-pettemer-sea-defence/

Hamilton S.E., and Casey D. (2020)
Creation of a high spatio-temporal resolution global database of continuous mangrove forest cover for the 21st century (CGMFC-21). *Global Ecology and Biogeography*, 25, 729–738. DOI:10.1111/geb.12449

IFRC and WWF (2022)
Working with nature to protect people. *Technical report*. https://www.ifrc.org/document/working-nature-protect-people

Johnson M., Goodlife R.J.W, Doygun G., Flikweert J. and Spaan G. (2020)
The UK's first sandscaping project. *Terra et Aqua*, 158. https://www.iadc-dredging.com/wp-content/uploads/2020/03/terra-et-aqua-158-complete.pdf

Karaliūtė V. (2021)
The valuation of externalities in maritime infrastructure projects. *Terra et Aqua*, 165. https://www.iadc-dredging.com/wp-content/uploads/2021/12/terra-et-aqua-165-complete-single.pdf

Spalding M.D., Ravitious C. and Green E.P. (2001)
World atlas of coral reefs. Prepared at the UNEP World Conservation Monitoring Centre. University of California Press, Berkeley, USA. https://wedocs.unep.org/handle/20.500.11822/30238

UNEP-WCMC, WorldFish Centre, WRI, TNC (2021)
Global distribution of warm-water coral reefs, compiled from multiple sources including the Millennium Coral Reef Mapping Project. Version 4.1. Includes contributions from IMaRS-USF and IRD (2005), IMaRS-USF (2005) and Spalding et al. (2001). Cambridge (UK): UN Environment World Conservation Monitoring Centre. DOI:10.34892/t2wk-5t34

Winterwerp J.C., Albers T., Anthony E.J., Friess D.A., Gijón Mancheño A., Moseley K., Muhari A., Naipal S., Noordermeer J., Oost A., Saengsupavanich C., Tas S.A.J., Tonneijck F.H., Wilms T., van Bijsterveldt C., van Eijk P., van Lavieren E., van Wesenbeeck B.K. (2020)
Managing erosion of mangrove-mud coasts with permeable dams – lessons learned. *Ecological Engineering*, 158. DOI:10.1016/j.ecoleng.2020.106078

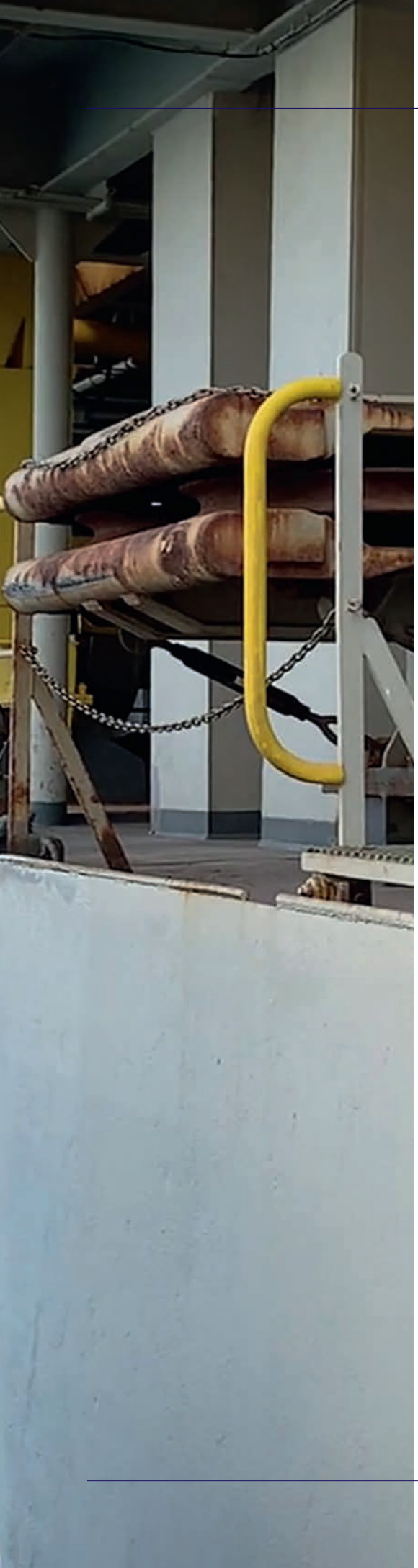

FINDING INNOVATIVE SOLUTIONS TO IMPROVE SAFETY

When individual employees, teams and companies view everyday processes and situations through a continuous lens of safety, they can each contribute to making all aspects of operational processes, whether on water or land, safer. For the 2022 Safety Awards, IADC's Safety Committee received 11 submissions. Each one is assessed on five different categories; sustainability; level of impact on the industry; simplicity in use; effectiveness; and level of innovation.

Affirming the importance of safety

Dredging activities can be risky operations with hidden dangers among heavy machinery. In response, the dredging industry proactively maintains a high level of safety standards. A representative of contractors in the dredging industry, IADC encourages its own members, as well as non-members participating in the global dredging industry, to establish common standards and a high level of conduct in their worldwide operations. IADC's members are committed to safeguarding their employees, continuously improving to guarantee a safe and healthy work environment and reducing the number of industry accidents and incidents to zero.

Recognising advancers of safety

IADC conceived its Safety Award to encourage the development of safety skills on the job and reward individuals and companies demonstrating diligence in safety awareness in the performance of their profession. The award is a recognition of the exceptional safety performance demonstrated by a particular project, product, ship, team or employee(s).

No submissions were received this year for the safety award granted to a supply chain organisation active in the dredging industry. This concerns subcontractors and suppliers of goods and services. In total, 11 submissions were received for the dredging contractor safety award. Each one aims to improve routine processes and situations encountered in the dredging industry. The winner will be announced during IADC's Annual General Meeting on 15 September 2022.

Dredging contractor safety award submissions

RETRACTABLE LADDER FOR TRACK EXCAVATORS BY DEME

Stepping on and off machinery is not without risks. Following an LTI, DEME carried out a thorough investigation and found a lot of operators had scars on their shins caused by contact with the tracks when stepping on and off track excavators.

The existing steps on an excavator are located inside the boundary of the tracks, which can be the cause of many injuries and near misses. Bringing the steps outside the tracks is not an option however, since this creates other risks both operational and for transport.

The solution – a retractable ladder that can be folded up just above the upper structure of the crane cabin. The area between the tracks and upper cabin stays completely free so there is no contact with sand or mud sticking on the tracks. Located on a safety area besides the excavator door, this innovative design needs almost no maintenance.

The ladder is made out of one piece of metal and retracts by itself after use. It can be positioned in the location of the original platform and both a bolted or welded connection is possible. The benefit of the design is that you only need one type of ladder. DEME foresee one standard ladder with a maximum length that can be adjusted to smaller track excavators.

HATCH SAFETY COVER BY JAN DE NUL

The hatch safety cover is a crew initiative that was built and installed on board Jan De Nul's trenching and offshore support vessel, Adhémar De Saint-Venant. Designed to increase safety on board, the cover ensures protection of the access ladder between decks. It prevents people falling through the opening and stops objects from falling down to lower decks.

It is a solution both easy to build, install and use. The design encompasses two vertical poles that remain in place and on which hinges are welded to hold the removable horizontal bars when the hatch is open. Chains attached to the permanent vertical poles are then connected to safely secure the hatch cover when opened. The horizonal bars can be stowed on hooks on the hatch cover when the hatch is closed.

Cost efficient, the hatch cover was built on board by the crew with available materials. The design can easily be adjusted to fit larger and smaller openings between decks, and can be implemented on any vessel.

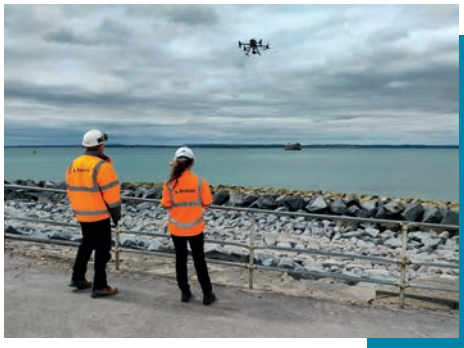

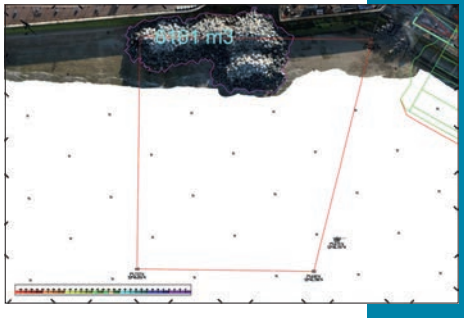

UNMANNED AERIAL VEHICLE (UAV) FOR SURVEYS BY BOSKALIS

During the South Sea Coastal Scheme (Sea Defence) project, Boskalis used an Unmanned Aerial Vehicle (UAV) for photogrammetry to fulfill the survey requirements of a coastal area. Use of the technology began in early 2017 and was introduced to the project in 2021. Over time, the team further developed and enhanced the ways of working. As confidence in the data improved, the project team substituted traditional survey methods for the new technology. Improvements in the technology also helped to improve the survey accuracy using the RTK (Real Time Kinematic) drone.

Use of an UAV presents many safety advantages. It eliminates field hours, thus reducing the time team members spend outside and therefore reducing the risk of trips and falls. Surveys can also be carried out away from uneven terrain and more importantly, away from potentially dangerous areas, for example, near heavy machinery or close to water.

Data collected allows the project management team to create an overview of the site on a regular basis. The final image is created from multiple photos stitched together into one orthomozaic image. This information helps support the project by acting as a daily planning tool for site activity and (sub)contractor coordination. It supports activities for safe design of work methods and collaboration on site, an indirect benefit for the project. In addition, the drone provides images of the status of the works, highly appreciated by the client.

Team members undertook a 5-day course to operate the drone and acquire the necessary licences from the local flight authority. Each drone flight is submitted to a website so that other drone flyers or stakeholders know when and where a drone is being deployed.

MANHOLE COVER BY DEME

During regular maintenance and inspections on board vessels, manhole covers are often removed to ventilate confined spaces below. During this ventilation process, a safety risk arises from the possibility of crew falling into the opened manholes.

To mitigate this risk and reduce the number of incidents, a manhole cover was custom-made using metal grating. A simple cross brace is then secured to the circular grate to hold the cover in place. The result is the ability to be able to ventilate confined spaces without the risk of falling incidents.

The custom-made covers can be made in the workshop on board any vessel. They are both inexpensive and easy to create, as well as easy to apply.

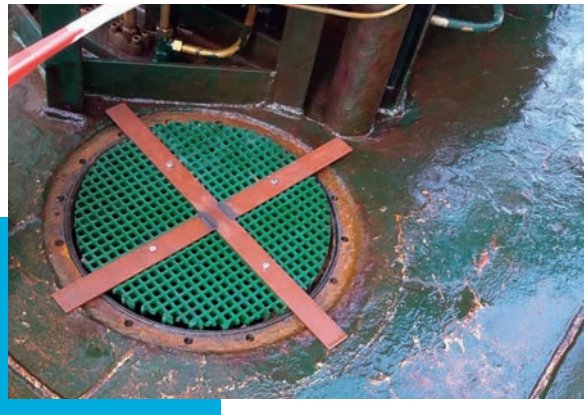

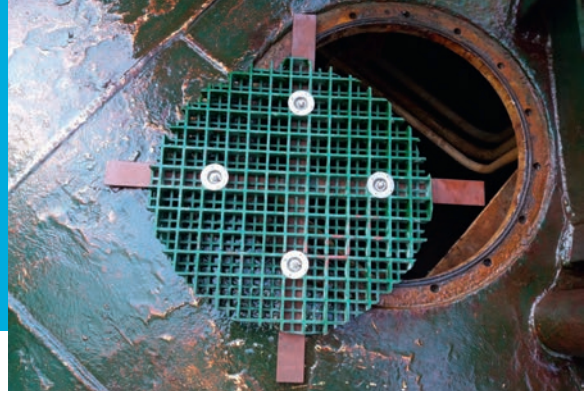

USE OF DAVIT CRANE FOR CABLE MANAGEMENT BY JAN DE NUL

During cutter head repair and other related welding works, electrical cables lay across workshop floors posing trip and fall hazards. The cables also often get damaged due to contact with metal plates, sharp objects and movement of other equipment on the workshop floor.

To address this issue, Jan De Nul adapted exisiting equipment to meet its needs. Instead of using the davit as a lifting device, it uses it to efficiently manage electrical and welding cables overhead. Able to rotate 180°, which makes them easy to use, the davit's swinging radius means the entire workshop area can be covered. Its use not only eliminates cables on the workshop floor, therefore reducing electrical risks and eliminating trip and fall hazards, it also protects cables from damage.

This significantly contributes to improve general housekeeping of the workshop area. From an ergonomic point of view, the davit bears the weight of the welding cables and thereby reduces the weight to be carried by the welder. This simple, cost-effective concept is a way of efficiently managing hazards as well as space management. The design can be used on all dredging vessels where hot work is carried out and in places where electrical and welding cables need be moved frequently therefore causing potential trip and fall hazards.

Future improvements include: increasing the capacity of the davit cranes so more welding cables can be used on each davit; applying a hinge in the middle of the davit crane to make it more mobile; and adding a gear system to keep the davit fixed in a desired position.

INSPECTION HATCH BY VAN OORD

Opening an inspection hatch in a suction line towards the pump is a frequent activity. Originally a bolted hatch, the opening of an inspection hatch is labour intensive. First, several nuts and bolts need to be loosened before lifting gear is then used to remove the hatch. After inspection, the same routine has to be carried out to close the hatch and enable dredging activities to continue.

Van Oord came up with a design to improve the existing bolted hatch to enable quick inspections, making the process less labour intensive and eliminating the need for lifting equipment. The new system uses a cantilever to allow the inspection hatch to be operated by a single person. It eliminates the need to use power tools to loosen nuts and bolts as well as the necessity to operate lifting gear, for example a deck crane, for removal and installation of the hatch.

The innovative application of this idea in this environment is both creative and unique; the use of this kind of cantilever in the suction line environment on board a vessel is not done at this scale and size of suction lines. The inspection hatch is currently installed on the suction pipe of Van Oord's new vessel, Vox Arianne. Extremely easy to use, the design can in principle be copied straight onto other vessels.

SEAGOING UNMANNED SURVEY VESSEL BY JAN DE NUL

Jan De Nul identified that smaller survey vessels, which were performing hydrographical measurements on coastal and shallow dredging areas, required a safer, greener and more cost-effective replacement. After carrying out extensive market research, the company decided upon a well-proven and hybrid Mariner Unmanned Surface Vehicle (USV) as the first step towards unmanned and autonomous survey operations.

The vessel, named Beluga 01, will be deployed worldwide for hydrographical and environmental surveys on marine and offshore construction projects. The Beluga 01 is based on the innovative Maritime Robotics' Mariner class USV, which for years has proven its mobility and seaworthiness for data acquisition under rough conditions. It is a user-friendly, cost-effective and low-risk platform for data acquisition at sea and serves as an alternative or addition to larger manned vessels.

By executing unmanned surveys, Jan De Nul fully commits to improving safety and operational control during its survey activities, to reducing carbon emissions and to acquiring data more efficiently.

IMPROVED TRAINING PROGRAMME BY NMDC

Since the dredging industry requires specific HSE information to be delivered to the workforce, NMDC developed customised training programmes based on the lessons learned from incidents, unsafe observations and health and safety data from internal and external sources.

New material for ten in-house training programmes was developed to include information related to the dredging industry. In addition, the company sent 13 HSE staff to follow the American National Standards Institute (ANSI) Train the Trainer course to gain accreditation from a world-leading accredited training body. ANSI was also asked to audit the entire training process including resources, trainers and course content before they accredited the ten programmes to ensure that all the required steps were fulfilled.

The company's 13 Train the Trainers are all from different nationalities with different dredging backgrounds to ensure the competency and understanding of its entire workforce. NMDC knows that by providing effective and comprehensive training programmes, employees' knowledge and skills systematically improve.

NMDC became the first dredging company to be accredited by ANSI National Accreditation Board (ANAB) for the training content it developed. Over the last 3 years, the training programmes have resulted in a reduction of incident individual factors by 50%.

TRUCK DE-TARPING STATION BY NMDC

A project scope involving the transport, reclamation and ground improvement of 10.2 million m³ of material presented NMDC with a challenge, from which came the design of a truck tarping station. With approximately 253,000 truck trips to the project location, the trucks needed to be covered with tarpaulin sheets to avoid sand blow out while in transit via public roads.

The traditional way of removing tarpaulin from the top of a truck involves the driver climbing to a height of 3 metres. Although a climbing ladder is fabricated within the truck for this purpose, the project team assessed the working at height risk as very high since the probability of occurrence was two times for each of the 253,000 trips.

To minimise this risk, NMDC's engineering team together with project team designed the de-tarping structure by utilising 40-feet shipping containers to provide a safe platform from which to carry out the procedure. Handrails provide a fall protection system around the platform and fixed stairs provide access. The platform height is the same level as the truck to avoid the de-tarping crew having to over reach. The platform structure is also equipped with lighting to allow safe operation during darkness and an overhead structure provides shelter from the elements.

Working in pairs with one worker deployed on each platform, a crew can remove the tarpaulin cover in just 3 minutes. The new safety design not only eliminates climbing on top of the truck but is more than three times faster than the original method. A red and green traffic signal is placed in front of each de-tarping bay and controlled by the crew on the platform. Once the tarpualin has been removed, the driver receives the green light that it's safe to move the truck. By implementing this new safety design, zero incidents related to truck de-tarping and working at height have been reported on the project.

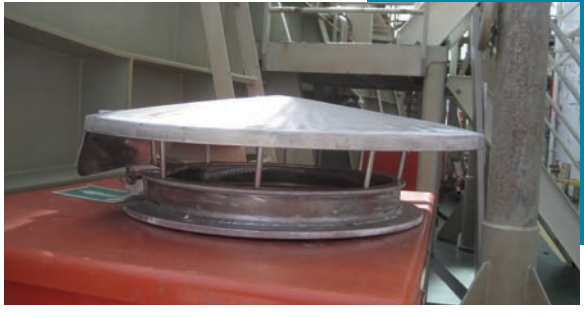

ROBIN HOOD COVER BY BOSKALIS

During repairs to vessels, which can take multiple days, the manhole covers on the weather decks need to be opened for tank inspections and ventilation. Usually, when it starts raining, a cement barrier is placed around the manhole to prevent water and dirt from flowing into the confined space and the opening is covered up. This is often not done however, resulting in the need for someone to go into the confined space to clean it.

To find a solution to this problem, Boskalis designed the Robin Hood; a manhole cover that can be opened and closed while preventing water ingress and enabling continuous ventilation of the tank. By using the Robin Hood, the tank stays clean during the repair period and the need for people to enter into the potentially dangerous area is limited to the bare necessity. When necessary, air hoses for forced ventilation of the confined space can be inserted between the bars of the manhole cover. As a result, the Robin Hood can still be closed (and opened), reducing the risk of confined space accidents.

Made from aluminium, the Robin Hood can be made to fit every type of tank cover. The cover is lockable when in the opened position to prevent it from falling shut. When in the closed position it both ensures proper ventilation while closing off access and preventing water ingress. Its durable material also means it can be used for many years.

SWINOUJSCIE-SZCZECIN FAIRWAY MODERNISATION BY DEME AND VAN OORD

After 2.5 million man-hours on the modernisation of the Swinoujscie-Szczecin Fairway in Poland, the project was completed with zero Lost Time Injuries (LTI's).

From the beginning in September 2018 until completion in March 2022, the team demonstrated exceptional safety performance through their commitment to the health and safety of themselves and everyone involved in the project. Safety became embedded within the project team, achieved through a systematic approach and the understanding that, as people, everyone is different and learns in different ways.

Simplified working processes and procedures were clearly communicated. The bridging of two management systems (DI & VO) to create one and the translation into the local language allowed for clear communication of the safety systems. Working together with so many cultures, nationalities and languages can present many challenges. However, through different forms of communication and understanding, everyone involved in the project found a common goal – to go home safe.

The clearing of hundreds of Unexploded Ordnances (UXOs) from WW2 within the active channel with zero LTI's also demonstrates not just the team's commitment but also the Polish Maritime Office's commitment to improving society's safety. The Szczecin works is a landmark project for Poland providing prosperity and development, and an enrichment of the environmental habitats. The reuse of dredge material to create nature habitats also adds greatly to the sustainability of the project and provides an environment for wildlife to thrive.

ESTIMATING SEDIMENT EROSION OF A CENTRIFUGAL DREDGE PUMP'S IMPELLER

Sediment erosion is a phenomenon of mechanical wear of components that decreases efficiency and uptime of the dredging process. Dredge pumps are designed to handle mixtures of water and solid particles with varying particle size from less than 0.002 mm to greater than 200 mm. A dredge pump's overall effectivity in the field depends upon its uptime. Uptime is influenced by the number of times the pumping process is interrupted, which can be due to maintenance combating the material loss, clogging, etc. This research deals with the erosion phenomena by considering a framework of numerical models, capable of qualitative and quantitative erosion estimation, coupled with experiments for validation. Coordinate Measurement Machine (CMM) is used for surface roughness measurement before and after the experiment, thus depicting the material loss due to erosion.

Centrifugal dredge pumps are used to continuously transport a mixture of soil and water through a pipeline. Material loss of the pump due to the flow is mainly caused by two ways: erosion due to solid particles in a flow (Figure 1) and erosion due to cavitation.

When the erosion rate of the pump components can be estimated in advance, i.e. during the design phase, the components can be altered such that the pump is more resistant to erosion wear (Krüger et al., 2010). This would allow reducing the maintenance costs of centrifugal dredge pumps. Another advantage of a reliable erosion estimation is the possibility to set up maintenance plans that show in detail when certain components have to be replaced. This will help to increase the efficiency of the dredging process.

The main objective of this research is to verify and validate the numerical model capable of estimating the sediment erosion wear due to slurry flow on the impeller blades of a centrifugal dredge pump by using Computational Fluid Dynamics (CFD).

Literature review

The flow field obtained from potential flow theory was used to calculate the particle velocities from a force or momentum balance in the early numerical models. Roco et al. (1985) and Roco and Addie (1987) used two-way coupling between the solid particles and the fluid. Although the method was limited to two-dimensional pump casings and inviscid flows, it showed reasonable agreement with experimental results. Ahmad et al. (1986) setup a three-dimensional model that included all slurry pump components.

It was assumed that the solid particles do not influence the flow field of the water (one-way coupling). In addition, a different erosion model was used that included the fact that the erosion wear is maximum when the particles leave the surface with zero tangential velocity. A validation study with experimental results showed that the model was able to estimate the location of maximum wear reasonably well while underestimating the level of erosion.

FIGURE 1

Effect of erosive wear on dredge pump. Photo © DAMEN.

More recently, Computational Fluid Dynamics (CFD) opened the doors for more sophisticated methods. Krüger et al. (2010) used an unsteady Eulerian-Eulerian model and found that the leading edge of the impeller blade suffers from erosive wear, with the maximum erosion in the middle of the leading edge. This was found to be due to the high turbulent kinetic energy close to the hub and shroud plates, which pushes the particles to the center. Along the blade, at the trailing edge and the side plate, abrasive wear dominates. To predict these phenomena accurately, it is important to accurately capture vortices and secondary flow structures in the impeller. Sapkota (2018) confirmed the occurrence of erosive wear at the leading edge and abrasive wear along the blade and near the trailing edge. In his study, based on a one-way coupled Eulerian-Lagrangian method in combination with Finnie's erosion model (Finnie, 1960), it was found that the maximum erosion occurs at the leading edge and on the pressure side near the trailing edge. When the flow rate is increased, the erosion on the blades also increases. Moreover, recirculation zones lead to an increased probability of particle impact. For further studies, the research recommended improving the model by using four-way coupled simulations.

Lai et al. (2018) found that an increase in concentration increases the erosion rate, due to particle impact frequency. On the other hand, it was shown that the particle diameter does not influence the particle trajectory and the impact frequency. These results came from computations with a transient two-way coupled Eulerian-Lagrangian model in combination with the E/CRC erosion model (Zhang et al., 2007). The transient nature of this model enabled it to show that the erosion rate first rises until a constant value is reached after about 0.5 seconds. Huang et al. (2019) confirmed the occurrence of the steady-state erosion rate using a similar model except for the erosion model. However, they showed that the time after which it is reached depends on the flow rate through the pump: for lower flow rates, the steady-state rate is reached later. Although Lai et al. (2018) showed that the particle diameter does not influence the particle trajectories, Tarodiya and Gandhi (2019), using a two-way coupled Eulerian-Lagrangian model, found that larger particle size are subjected to higher kinetic energy, thus, increasing the erosive wear. In addition, they found that increasing the concentration of the sand particles increases the wear, and lowering the pump speed leads to a reduction in wear.

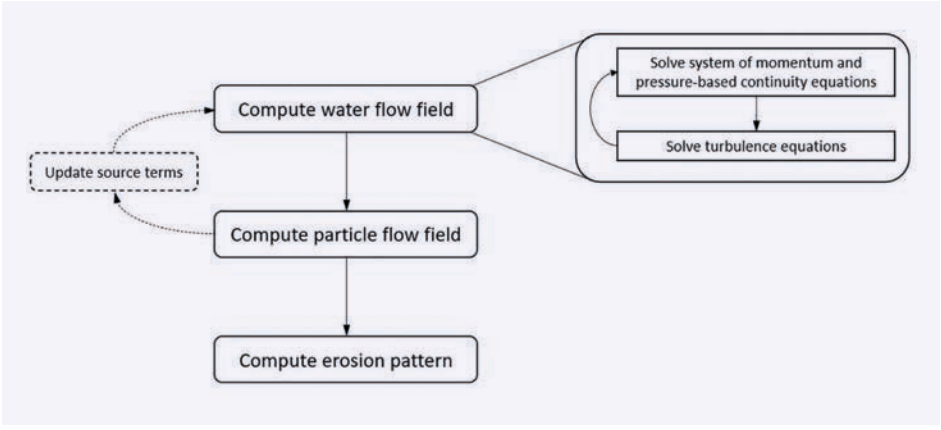

FIGURE 2

Schematic overview of the numerical models. The dashed part of the figure is only included for the two-way and four-way coupled methods.

Xiao et al. (2019) accounted in their study the change in geometry of the blade profiles due to wear by using a two-way coupled Eulerian-Lagrangian model. Qualitatively, the results of this model agreed with experiments, which were part of the study. By taking the geometrical changes into account, the unsteady behavior of the problem could be studied. This showed that the impeller blade degrades first, which enhances recirculation. Due to a combination of this recirculation and increased clearances, the wear at the impeller outlet, the bottom of the impeller blade and the volute casing decrease. Therefore, they concluded that small geometrical changes (for instance, due to erosion wear) change the later erosion patterns.

Several studies have already been conducted on the subject of erosion modelling for centrifugal dredge pumps. It was found that CFD can be used to compute the erosion pattern in a qualitative way (Krüger et al., 2010; Tarodiya and Gandhi, 2017), whereas the existing methods lack accuracy on a quantitative level.

Numerical model

The erosion occurring in centrifugal dredge pump impellers is modelled using the CFD package ANSYS Fluent version 2020 R2.

Water flow field

Following the Einstein convention, the governing equations (continuity and momentum) of incompressible flows after applying the Reynolds decomposition are given below (Nieuwstadt et al., 2016).

Here ρ is the fluid density, $\bar{U}$ is the averaged ensemble of the fluid velocity vector. For the turbulence equations, the k-ω SST turbulence model is used. The right side of the equation consists of the isotropic stress due to the mean pressure field ($\bar{P}$), the mean body force ($\bar{f}$), viscous stress and averaged Reynolds stress tensor ($-\rho\overline{U'_i U'_j}$) due to the fluctuating velocity field, respectively. There are various turbulence models available to convert the Reynolds stress into mean quantities and ensure closure.

k-ω SST turbulence model (Menter, 1994) is followed in the current study based on the study from Wang and Wang (2012) and Ilker and Sorgun (2020).

$$\frac{\partial \bar{U}_j}{\partial x_j} = 0 \qquad j = 1,2,3 \tag{1}$$

$$\rho\left[\frac{\partial \bar{U}_i}{\partial t} + \frac{\partial(\bar{U}_i\,\bar{U}_j)}{\partial x_j}\right] = -\frac{\partial \bar{P}}{\partial x_i} + \rho\bar{f}_i + \mu\frac{\partial^2 \bar{U}_i}{\partial x_j \partial x_i} - \rho\frac{\partial \overline{U'_i U'_j}}{\partial x_j} \qquad i,j = 1,2,3 \tag{2}$$

$$m_p \cdot \frac{dU_{i,p}}{dt} = F_{i,Drag} + F_{i,Buoy} + F_{i,Virt} + F_{i,Press} + F_{i,Rot} + F_{i,TD} \qquad i = 1,2,3 \tag{3}$$

Particle flow field

After obtaining the converged fluid flow field, the particle flow field is calculated using Newton's second law for sets of particles, named parcels.

m_p is the mass of the particle, equal to $m_p = (\pi d_p^3 \rho_p)/6$. In addition, the subscript i refers to the vector component according to the Einstein notation and the subscript ρ is used for quantities related to the particle. The terms on the right-hand side represent the forces acting on the particle.

The first force that is considered here is the drag force (ANSYS Inc., 2020a).

$$F_{i,Drag} = \frac{1}{2} * C_D * \rho_F * A_p ||\vec{U}-\vec{U}_p||(U_i - U_{i,p}) \quad i = 1,2,3 \qquad [4]$$

A_p is the projected area of the particle normal to the flow (equal to $\pi d_p^2/4$). In addition, the term C_D is the drag coefficient, for which various models exist. For smooth, spherical particles, a general law called the Spherical Drag Law can be used (ANSYS Inc., 2020a):

$$C_D = K_o + \frac{K_1}{Re_p} + \frac{K_2}{Re_p^2} \qquad [5]$$

Re_p is the particle Reynolds number $Re_p = \rho d_p ||\vec{U}-\vec{U}_p||/\mu$. K_o, K_1 and K_2 are the constants that have to be determined empirically.

The buoyancy force due to the difference in the density of the particle and fluid is given by (ANSYS Inc., 2020a):

$$F_{i,Buoy} = V_p g_i (\rho_p - \rho) \qquad [6]$$

V_p is the volume of the particle.

When the particle accelerates through a fluid, a portion of the fluid is accelerated with it. This can be modelled as an additional mass that is quantified by virtual mass force (Andersson et al., 2012):

$$F_{i,Virt} = -C_{VM} * m_F * \left(\frac{DU_i}{Dt} - \frac{dU_{i,p}}{dt}\right) \quad i = 1,2,3 \qquad [7]$$

For the fluid acceleration, the substantial or Lagrangian derivative D/Dt should be used (Crowe et al., 1998). The virtual mass factor C_{VM} is often set equal to 0.5.

Equation 8 quantifies the pressure force acting on the particle. It is assumed that the pressure and shear stress do not change over the volume of the particle (Andersson et al., 2012).

$$F_{i,Press} = V_p\left(-\frac{\partial P}{\partial x_i} + \frac{\partial \tau_{ij}}{\partial x_j}\right) \quad i,j = 1,2,3 \qquad [8]$$

The rotational forces arise from rotating frames of reference (ANSYS Inc., 2020a). It includes the Coriolis (first term) and centrifugal forces (last term) and it correlates to (Sapkota, 2018):

$$\vec{F}_{Rot} = m_p(-2\vec{\Omega} \times \vec{U}_p - \vec{\Omega} \times (\vec{\Omega} \times \vec{R})) \qquad [9]$$

In this equation, $\vec{R}$ is the position vector. In the current study, the Discrete Random Walk model is adopted for the turbulent dispersion force.

Particle-wall rebound

Grant and Tabakoff (1975) proposed an empirical model for the restitution parameters (e) (ratios of normal (subscript N) and tangential (subscript T) velocities before and after the collision) with a dependency on the particle impact angle (in radians).

$$e_N = \frac{U_{N_2}}{U_{N_1}} = 0.993 - 1.76\alpha + 1.56\alpha^2 - 0.49\alpha^3 \qquad [10]$$

$$e_T = \frac{U_{T_2}}{U_{T_1}} = 0.988 - 1.66\alpha + 2.11\alpha^2 - 0.67\alpha^3 \qquad [11]$$

Particle-particle interaction

By using an additional extension of the model, the four-way coupled method is obtained. Here, also the forces due to inter-particle collisions are taken into account when calculating the particle flow field. This is done using the linear soft sphere collision model (also known as the DEM model). In this model, the forces in normal and tangential directions are split. In the normal direction, the collision is modelled as a spring system. This spring system can either be linear or non-linear. For the former, the force induced by the collision is equal to (ANSYS Inc., 2020a):

$$\vec{F}_{normal} = K_s \delta \vec{e}_{12} = \frac{\pi \left|\left|\vec{U}_{p,2} - \vec{U}_{p,1}\right|\right|^2}{3\varepsilon_D^2} D_{parc}\, \rho_p \delta \vec{e}_{12} \qquad [12]$$

In this equation, K_s is the spring constant, δ is the overlap of the parcels (or particles) and ε_D is the fraction of the diameter that is allowed to overlap. In addition, D_{parc} is the diameter of the colliding parcels and $\vec{e}_{12}$ is the unit vector between the two colliding parcels (or particles). In tangential direction, Coulomb's friction law gives (ANSYS Inc., 2020a):

$$\vec{F}_{friction} = \mu_{coll}(U_r)||\vec{F}_{normal}|| \qquad [13]$$

In Equation 13, the friction coefficient $\mu_{coll}(U_r)$ has to be determined through literature or experiments.

Erosion model

The Oka erosion model is used which takes into account the impact angle, particle size, material hardness, and velocity of the individual parcels hitting the target surfaces (Oka et al., 2005a). The model calculates the erosion rate in terms of volume ER_v from the same erosion rate at an impingement angle of 90 degrees.

$$ER_v = ER_{v,90} f(\alpha) \qquad [14]$$

$$f(\alpha) = \sin^{n_1}(\alpha)[1 + H_v(1 - \sin(\alpha))]^{n_2} \qquad [15]$$

This impact dependent function includes two coefficients (n_1 and n_2) and the material Vicker's hardness H_v. The coefficients themselves also depend on the hardness of the target material (Oka et al., 2005a). In this equation, the constants K, k_1 and k_3 depend on the particle properties, whereas k_2 is determined both by the material hardness and the particle properties. Moreover, a and b are empirical coefficients. The quantities U^* and d^* are the standard impact velocity and the particle diameter, which were used in the experiments for the determination of the erosion correlations (Oka et al., 2005b).

$$ER_{v,90} = K(aH_v)^{k_1 b}\left(\frac{U_p}{U^*}\right)^{k_2}\left(\frac{d_p}{d^*}\right)^{k_3} \qquad [16]$$

Experimental setup

For the experiments, a facility is used that is operational and available with the company Damen Dredging Equipment. This circuit is known as the "test loop" and can be seen in Figure 3.

Starting from the dredge pump (Figure 3), the mixture flows through the vertical U-bend and a horizontal 180-degree bend. After encountering a long horizontal pipe and another 180-degree bend, the flow enters a section with a density and a flow meter.

During the erosion experiment, Dredge Gate Valve 2 (DGV2) is closed, which allows the mixture to flow directly back to the dredge pump. Therefore, during the experiments, the circuit is a closed-loop system. When DGV2 is opened, the mixture can be forced through the hopper or the dump pipe that allows the user to control the sand concentration within the circuit. Since the conditions used by Sadighian (2016) are similar to the conditions in the current study, it is expected that, by refreshing the sand about every 9 hours, the effect of particle degradation is minimised.

Erosion measurement

For the quantification of the erosion wear, a Coordinate Measurement Machine (CMM), CRYSTA-Apex S1200 series model, is used. This device measures the x-, y-, and z-coordinates (relative to a reference frame defined on the object) of discrete points that are located on the surfaces of the measured object (Keyence Corporation, 2021). These points can either be measured using a contact probe or an optical probe. The theoretical accuracy of the machine is defined as $Accuracy=2.3+0.3*(L/1000)\ \mu m$. L is a measure for the size of the object in millimeters. In practice, the accuracy also depends on factors related to the state of the object, such as the roughness. Therefore, the practical accuracy will generally be lower than its theoretical counterpart ($0.1\ \mu m$) (Mitutoyo Corporation, 2021).

The thickness loss due to erosion wear at the different measurement points can be found by comparing the CMM measurements of the impeller before and after the wear experiment. For this, the CMM can be programmed such that it measures the same profiles during both measurements. A limitation associated with the CMM was that it was not able to measure the entire blade due to the absence of a longer optical probe. More specifically, the leading edge and a part of the suction side of the blade are not included in the experimental erosion results as the shorter contact probe was not able to measure the areas close to the aforementioned surfaces. In addition, the parts of the blade that are close to the hub and shroud of the impeller are not measured.

Experiment specifications

Parameters	Values
Pump parameters	
Inlet diameter of impeller	250 mm
Outlet diameter of volute	250 mm
Diameter of impeller	635 mm
Width of impeller	180 mm
Number of blades	3
Material of the impeller	Bainitic nodular cast iron
Density of impeller material	7800 kg/m³
Vickers hardness of impeller material	3.54 GPa to 3.98 GPa (Markus, 2020)
Best Efficiency Point (BEP) Conditions	
Flow rate, Q_{REP}	0.208 m³/s
Mean velocity, $U_{mean,BEP}$	4.24 m/s
Head, H_{REP}	20.75 m
Power, P_{REP}	55 W
Rotational rate, N_{REP}	10 1/s
Experiment conditions average over time	
Mean flow velocity during experiment, $U_{mean,exp}$	4.301 m/s
Rotational rate, N_{exp}	9.94 1/s
Concentration of sand, C_{vs}	9.94%
Mean particle diameter, d_{50}	0.619 mm
Time duration of the experiment*	55,7 hours

TABLE 1

Parameters for the experiment. *Time to start and stop the system are not taken into account.

Results

Benchmark study: Impinging jet

Two separate studies are used for the benchmark study and thus two sets of grid independent studies for flow field and erosion validation respectively. The fluid and particle flow fields are validated using the experiment by Miska (2008), whereas the validation of the resulting erosion pattern is performed using the research conducted by Wang et al. (2021) (Figure 5). For measuring the velocity field, the Laser Doppler Velocimetry (LDV) technique was adopted by Miska (2008).

Since the flow rate through the nozzle is known, a constant velocity is specified at the inlet of the nozzle by using a "velocity inlet" boundary condition. The inner and outer sides of the nozzle, as well as the target surface, are described by the "no-slip wall" boundary condition. The part of the outer diameter that is closest to the wall is defined as a "pressure outlet", whereas for the remaining sides of the domain the "pressure inlet" boundary condition is used to allow for entrainment.

Flow field validation

The first step in the validation of the fluid flow field consists of a grid convergence study. For quantifying the grid convergence, the pressure averaged over the target surface is used as the scalar quantity. From this quantity, calculated for the three finest grids, an observed order of accuracy equal to 1.7 was obtained (Celik et al., 2008).

In Figure 6, the fluid flow fields as calculated with the four grids are compared with the experimental results of (Miska, 2008). This is done using the velocity profiles at four different locations as indicated by red lines. When comparing the numerical to the experimental results, the top two graphs in Figure 6 show that the axial velocity in the middle of the jet is computed accurately. In addition, in Figure 7 (bottom right), it can be seen that the numerical radial velocity profile away from the center of the domain is close to the experimental profile. On the other hand, directly behind the nozzle wall, the axial

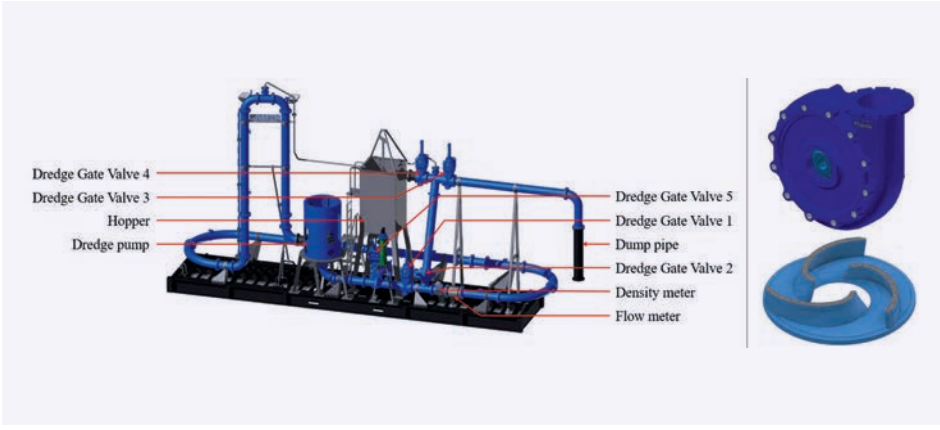

FIGURE 3

The "test loop" facility with 3D-model and cross-section of the centrifugal dredge pump (top right) and impeller (below).

FIGURE 4

Coordinate Measurement Machine (Mitutoyo Corporation, 2021)ρ

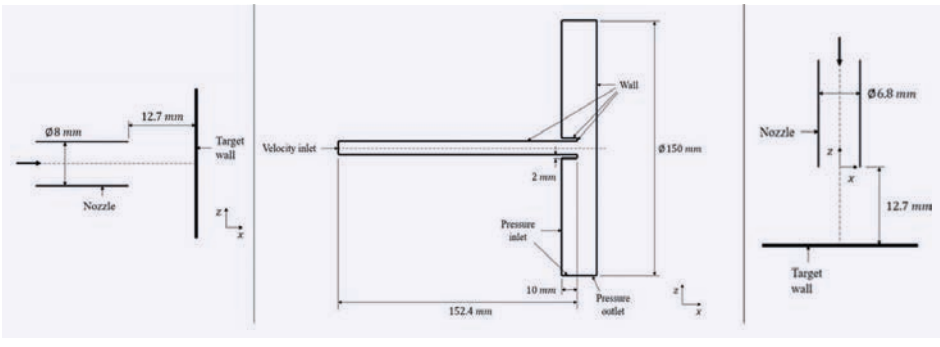

FIGURE 5

Left: Experimental setup for the submerged impinging jet as used in the study of Miska (2008). Centre: Cross-section of the computational domain for the flow field benchmark. Right: Experimental setup for the submerged impinging jet used in the study of Wang et al. (2021).

Parameters	(Miska, 2008)	(Wang, et al., 2021)
Nozzle diameter	8 mm	6,8 mm
Particle material	Aluminium	Sand
Density of particle	2650 kg/m³	2650 kr/m³
Flow rate of the jet	1.82 m³/h	1.83 m3/h
Diameter of particles	3µm and 120 µm for water and particle flow field study, respectively	80,5 µm
Concentration, C_{ys}	0,03%	1%
Target surface material	-	Stainless steel 316
Target material density	-	7980 kg/m³
Hardness of the material	-	1.795 GPa

TABLE 2

Specifications for the benchmark study.

velocity is overpredicted, especially near the sides of the profile. In addition, in line with the nozzle wall, there is a noticeable difference between the numerical and experimental profiles for the radial velocity due to the highly curved streamlines in that region.

Influence of the particles on the water flow field

In the second phase of the experimental study by Miska (2008), the small particles ($3\ \mu m$ diameter) were replaced by aluminum particles with a mean diameter of $120\ \mu m$.

The first step in the validation of the particle flow field is to verify whether these results converge to a certain solution while refining the grid. By comparing the numerical to the experimental results, it turns out that the axial and radial particle velocity is overpredicted and underpredicted respectively (Figure 7). The latter is caused by the underprediction of the radial water velocity at those locations.

Erosion validation

In the second part of the benchmark study, the numerical erosion is compared to the results of the experiment conducted by Wang et al. (2021). Since the domain of Wang et al. (2021) is slightly different, there is a need for another set of grid convergence studies. For the next set of grid convergence tests (Figure 8), the order of accuracy was found to be 1.8 for the average pressure around the target surface (Celik et al., 2008).

The erosion is quantified in terms of the thickness loss rate in $\mu m/s$. The x-coordinate is non-dimensionalised by using the radius of the nozzle. Since the increase in

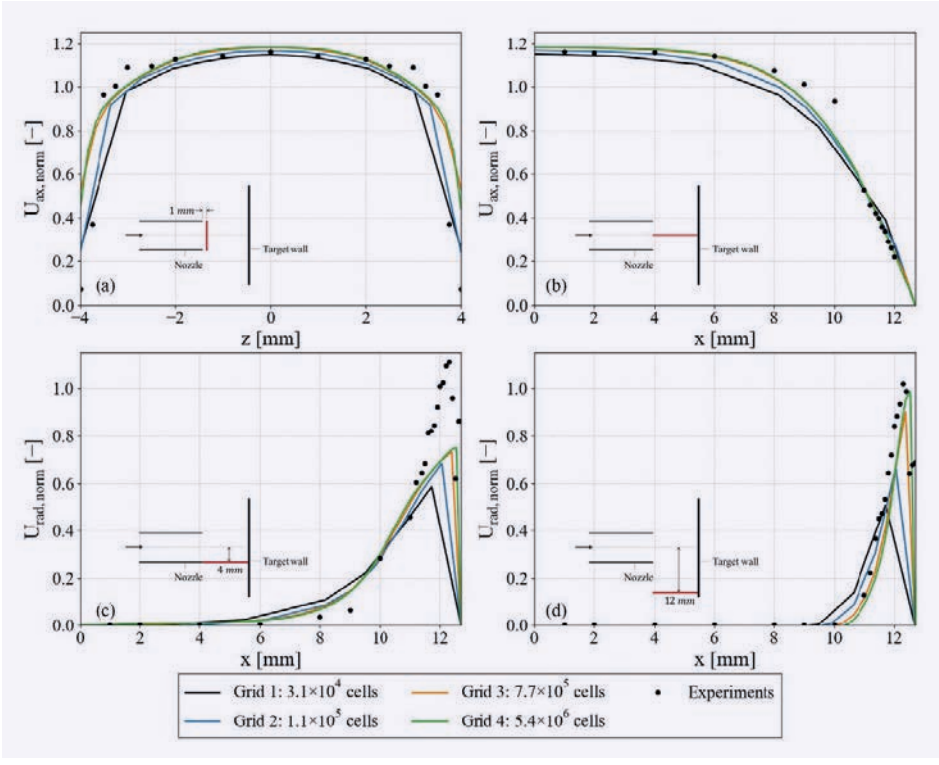

FIGURE 6

Comparison of the numerical results, as computed using different grids, with the experimental fluid velocity ρeld for different profiles (Miska, 2008). The red lines indicate the locations of the velocity profiles.

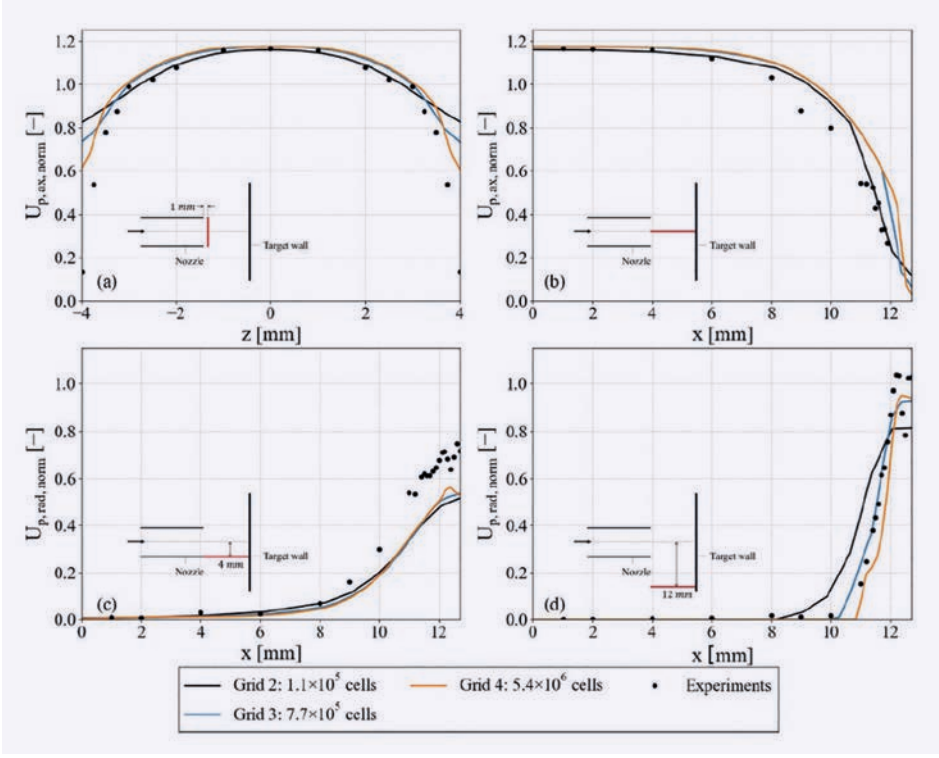

FIGURE 7

Comparison of the two-way coupled numerical results, as computed using different grids,

computational effort of grid 4 with respect to grid 3 is considerable, grid 3 is considered to be sufficiently refined. Therefore, this grid is used for the comparisons in the following paragraphs.

The minimum amount of erosion can be found directly in line with the centerline of the nozzle. This is due to the particle velocity being (almost) equal to zero as was also demonstrated for the flow field benchmark. When moving away from the center of the target surface, the erosion rate increases until it reaches its peak around $x = 1.5 * r_{nozzle} = 0$. This implies that the erosion peak occurs outside the nozzle diameter projected on the target surface.

The magnitude of the erosion peak is largely overpredicted. For the specific type of stainless steel that was used by Wang et al. (2021), hardness values as high as 3.687 GPa can be found. In Figure 9, the resulting erosion profile for this hardness is compared to the erosion profile obtained with a hardness equal to 1.795 GPa. Although the larger hardness still involves a certain error, changing the hardness does have a significant effect.

Sensitivity tests: Coupling

In Figure 10, the erosion profiles for the different coupling methods are compared. In addition, to illustrate the dependency of the four-way coupled method on the parameters of the collision model, the resulting profile for this method is shown for two different values of the static friction coefficient μs.

While the profile for $\mu s = 0.5$ is closer to the one-way coupled result, the profile for $\mu s = 0.05$ is similar to the profile that is computed with the two-way coupled solver. This large difference can be attributed to the loss in kinetic energy of the particles due to the friction; for a higher friction coefficient, the velocity of the particles near the wall decreases considerably as compared to the situation with a small friction coefficient. For the four-way coupled solver to be accurate, the accurate values of the parameters from this collision model should be obtained (either from literature or from conducted experiments).

Sensitivity tests: Erosion model

To verify the choice of the Oka erosion model for this specific situation, a comparison is performed that includes the different erosion models, which is considered to have a similar

performance as the Oka model (Zhang et al., 2007). In addition, the Finnie erosion model is included since this model is often used in literature.

For all the profiles, the erosion is the smallest in the middle of the target surface. The erosion rate increases until it reaches its peak around $x = 1.5 * r_{nozzle} = 0$. This location is predicted well by all the considered erosion models. Quantitatively, however, there are large differences between the results. Finnie's model does not take into account the size and shape of the solid particles. This introduces additional uncertainties in the model. For the E/CRC model, similar reasoning can be given as for the Finnie model. Zhang et al. (2007) showed that the parameters that are used in the E/CRC model were developed with experimental data using the material Inconel 718 and do not take into account the diameter of the particles.

Impeller model

Verification

By making use of the symmetry within the impeller, only one of the three blades is included. To this end, two periodic faces are defined with a rotational symmetry boundary condition. The domain contains four different walls, the hub, the shroud, the blade and the pipe (all walls are defined with the no-slip condition). In addition, the flow enters the pipe through a velocity inlet condition and exits the impeller via a pressure outlet. The impeller walls rotate with the same rotational velocity as the domain. For this, the computational domain is displayed in Figure 12.

For the grid convergence study, three different grids are constructed that are geometrically similar. For this, the parameters that are listed in Table 3 are used. It can be seen that for all three grids, the first cell height is larger than the particle diameter that is used in the computations. This results in a y^+ for all three grids within the range of the applicability of wall functions. Although flow separation is expected to occur from the impeller blades, it is not possible to refine the near-wall region further, since this would compromise the computations of the particle paths. In Figure 13, the different grids around the impeller blades on a y-z plane are displayed.

For the quantification of the grid convergence, the head of the pump can be used. This parameter is the total pressure difference

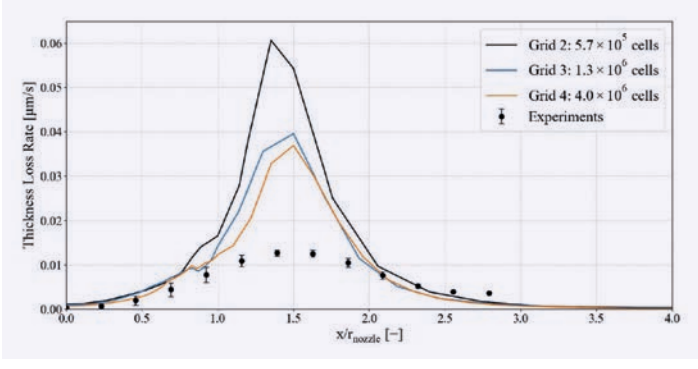

FIGURE 8

Comparison of the erosion profile, as computed using the two-way coupled method for different grids, with the experimental erosion profile at the target surface (Wang et al., 2021). The center of the domain is located at $x = 1.5 * r_{nozzle} = 0$.

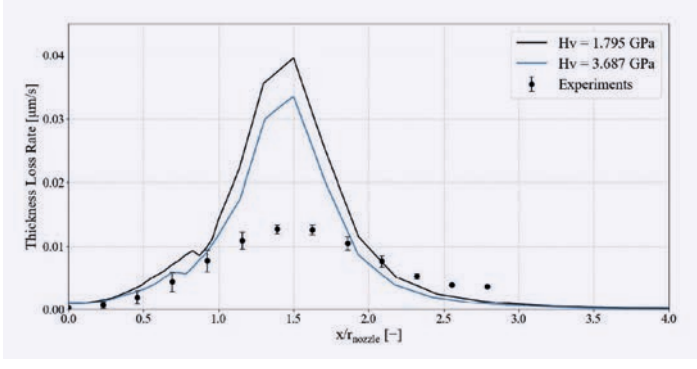

FIGURE 9

Comparison of the erosion results, as computed using the two-way coupled method for different values for the hardness (Wang et al., 2021). The center of the domain is located at $x = 1.5 * r_{nozzle} = 0$.

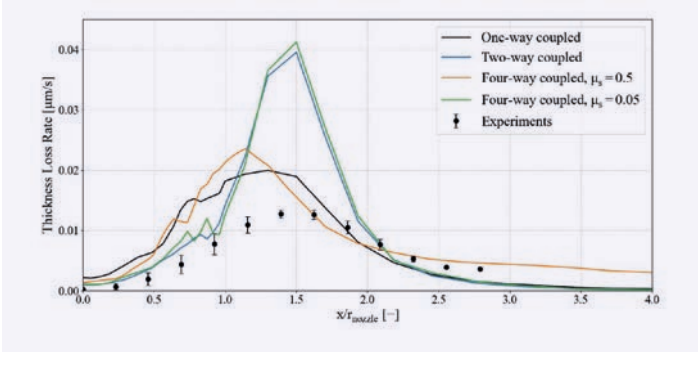

FIGURE 10

Comparison of the erosion results using the different coupling methods (Wang et al., 2021). The middle of the domain is located at $x = 1.5 * r_{nozzle} = 0$.

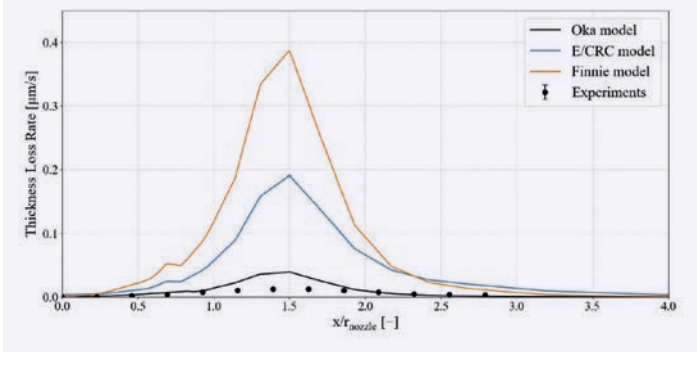

FIGURE 11

Comparison of the erosion results, as computed using the two-way coupled method in combination with different erosion models (including the results of the experiments by Wang et al. (2021). The middle of the domain is located at $x = 1.5 * r_{nozzle} = 0$.

Grid	Δx [mm]	First cell height blade [mm]	Number of cells	$y^+_{avg\ blade}$ [-]
Grid 1	5.17	1.57	$8.48 * 10^5$	132.5
Grid 2	3.76	1.10	$2.19 * 10^6$	77.6
Grid 3	3.02	0.85	$4.26\ 8\ 10^6$	53

TABLE 3

Grid parameters used in the grid convergence study for the impeller.

between the outlet and the inlet of the impeller. The resulting relative error is displayed as a function of the typical cell size in Figure 14. Since the convergence of computations on the two finest grids is such that there is still a variation in the head of about 1%, the head that is used to calculate the relative error is averaged over the last 200 iterations.

To verify the grid convergence on a local scale, the pressure along the blade is shown in Figure 15.

In Figure 15, the position on the blade is non-dimensionalized using the chord length(c) of the blade. Therefore, the leading edge can be found at $x/c = 0$, whereas the trailing edge is located around $x/c = 1$. It can be seen that the difference between the results becomes smaller with an increasing number of cells. However, the difference between grids 2 and 3 is still relatively large, which is also visible in Figure 15. From the discussion in this paragraph, it can be concluded that grid 3 is the best option to base the erosion calculations on. However, it turned out that on the two finest grids, the particle tracking computations using the two-way coupled method could not be converged. Therefore, in the following paragraphs, the coarsest grid is used.

Validation of the erosion model

In the previous section, a comparison between different erosion models is performed for the impinging jet benchmark. In this paragraph, the same analysis is done for the impeller. Here, erosion models like the Oka, Finnie and the E/CRC are compared with the experimental results. Only the part of the blade where the erosion was measured is shown in Figure 16.

It can be seen that the erosion values predicted by the E/CRC model are much larger than those for the experiment as well as for the other erosion models. This large overprediction may be due to the fact that the model was designed for high particle velocities in combination with rather small particle diameters. In addition, the material that was used during the experiments was Inconel 718. Therefore, it may be that the applicability of the model is restricted to situations that are more similar to the design conditions than the conditions used in the current project.

The differences between the Oka and Finnie erosion models are much smaller. While there is a slight underprediction in Figure 16 of the erosion rate at the suction side of the blade by the Oka model, the Finnie model predicts a higher erosion rate than the experimental value at the same location. The reason for this is that the Finnie model predicts the maximum erosion for a lower impingement angle than the Oka model. This is visualised in Figure 17.

The erosion that occurs in the region that is shown in Figure 16 is mostly due to sliding wear corresponding to the study of Krüger et al. (2010). Therefore, the differences in results for the Finnie and the Oka erosion models are due to the different angle dependencies of the two models. In the specific profile that is shown in Figure 16, the Oka model is closer to the experimental results. However, in other regions, the Finnie model corresponds better to the experiment. Therefore, for the validated region, the models perform equally well. However, at regions where the impact wear is dominant (for instance at and near the leading edge of the blade) it is expected that the prediction of the Oka model is much closer to reality than

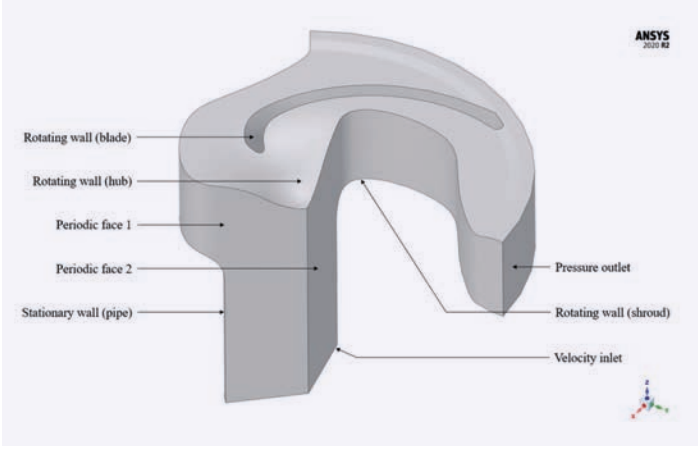

FIGURE 12

Numerical domain for the impeller computations.

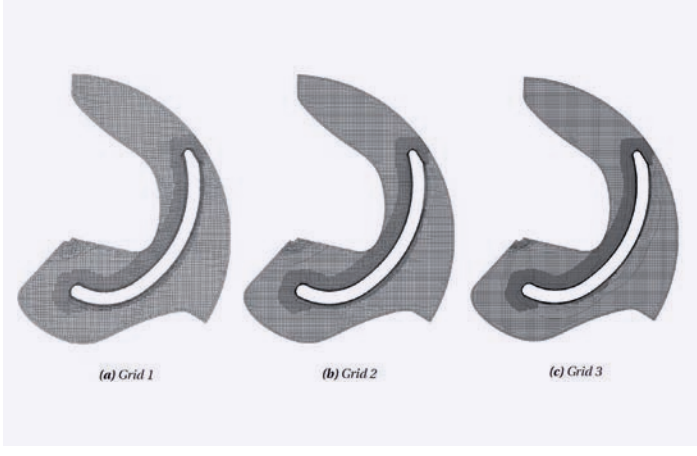

FIGURE 13

Cross-section of the different grids that are used for the impeller grid convergence study.

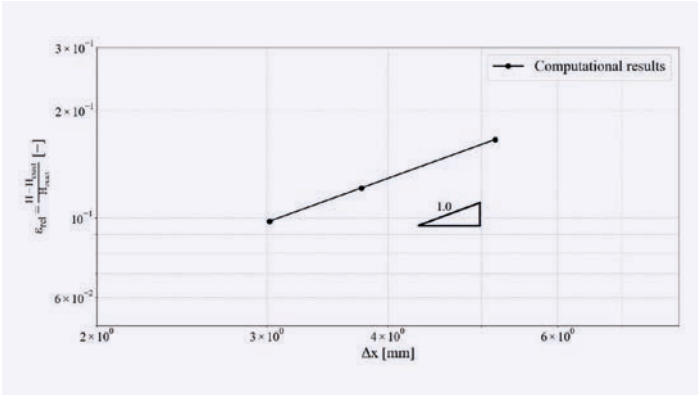

FIGURE 14

Relative error (based on the head) for the impeller computation as a function of the typical cell size.

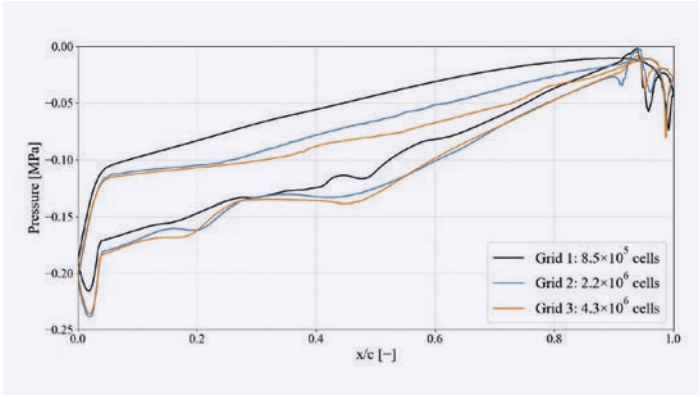

FIGURE 15

Comparison of the pressure distribution along the impeller blade for the different grids.

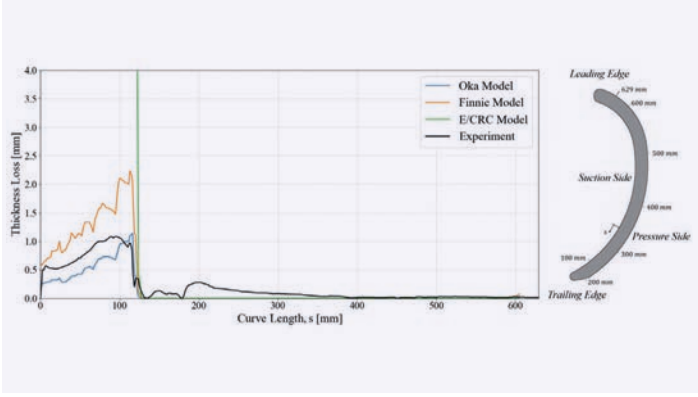

FIGURE 16

Erosion profile along the blade for different erosion models (including the results of the experiment. On the right-hand side of the figure, the definition of the curve length *s* is shown.

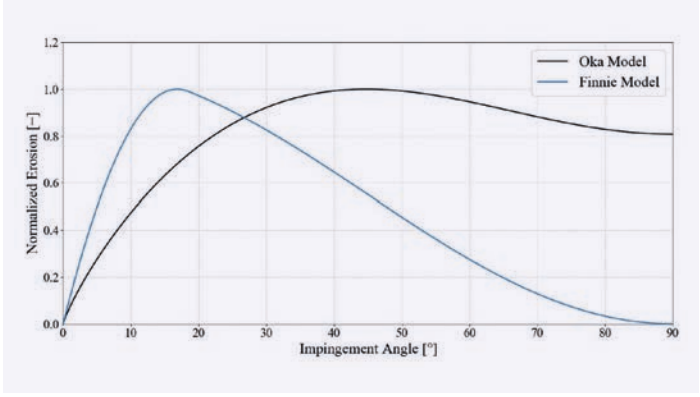

FIGURE 17

Normalised erosion as a function of the impingement angle.

that from the Finnie model. This is because the Finnie model yields an underprediction of the erosion rate for impact angles larger than 45 degrees. Moreover, Figure 17 shows that at a 90-degree impact angle, the Finnie model predicts no erosion at all. Therefore, it can be concluded that the Oka model is more suitable for computing the erosion in a centrifugal dredge pump impeller than the Finnie model.

In Figure 18 and 19, the numerical and experimental results are compared. For the former, the two-way coupled method result on the coarsest grid (Table 3) is used. The suction side and trailing edge of the blade are shown in Figure 18.

When comparing the erosion values at the suction side of the blade, it can be seen that the erosion profiles correspond well qualitatively. The magnitude of the erosion increases when moving towards the trailing edge of the blade. In addition, the erosion increases in the direction of the shroud. Quantitatively, however, there is an underprediction of the erosion values at the suction side of the blade by the numerical model. One explanation for this would be that a constant particle diameter was used in the numerical model, while the PSD showed a large spread of particle diameters as used during the experiment. Since the gravitational acceleration acts in the positive x-direction, neglecting the smaller particles results in more particles moving towards the shroud. Especially since the densimetric Froude number for this situation is equal to 4.4, which indicates that the effect of gravity cannot be neglected. Another explanation would be that the recirculation zone that is causing the erosion at the suction side is smaller in reality than that is calculated. Since the recirculation zone is a complex phenomenon to capture, the strength of the vortices within the recirculation zone may be larger in reality than in the calculation. This leads to an underprediction of the impingement velocity and volume fraction at the blade.

The trailing edge of the blade shows that the erosion at that location is underpredicted. According to the numerical model, there is only erosion at the part of the blade close to the shroud, while the experiment showed erosion over the entire height (in the x-direction) that was measured. This discrepancy can be explained by looking at the fact that the flow separates from the blade somewhere

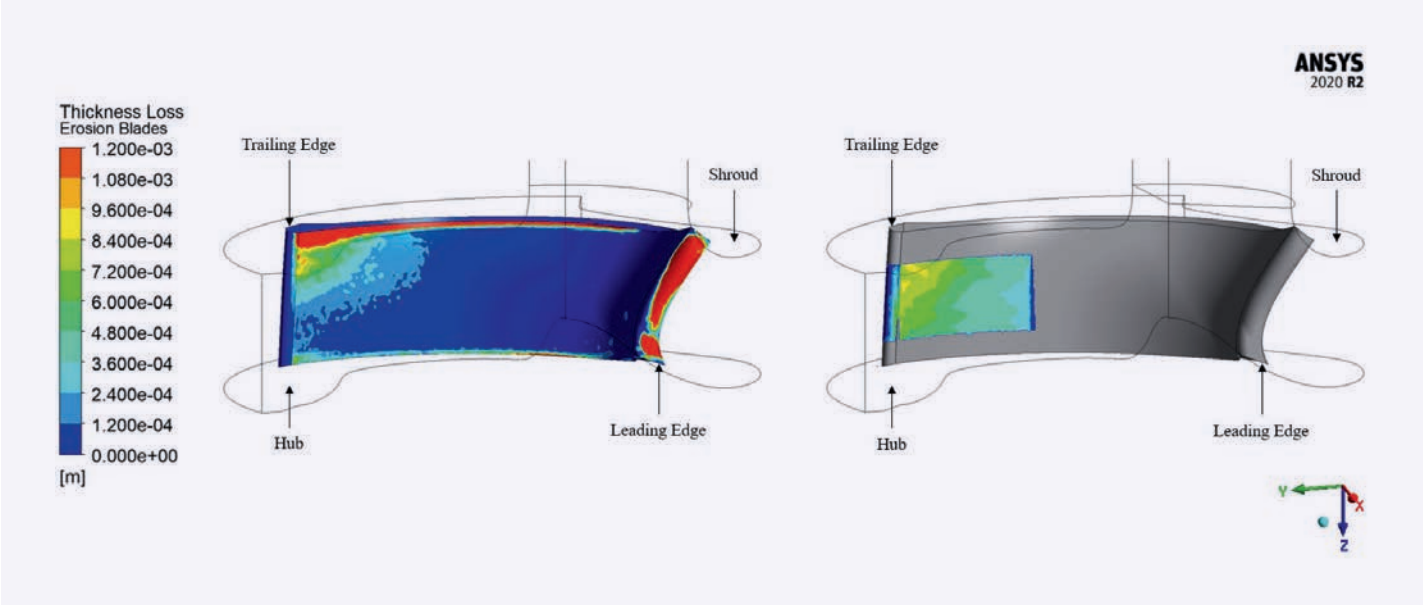

FIGURE 18

Erosion pattern on the suction side and the trailing edge of the blade for the two-way coupled numerical model (left) and the experiment (right).

at the trailing edge. Keeping in mind that the numerical model that is used in this study is not capable of calculating large separating flows, it cannot be expected that the model captures the flow well at that region.

The third region that was measured during the experiments is the pressure side of the blade. The comparison between the numerical and experimental results for this side is shown in Figure 19. On the pressure side, only a small (relative to the erosion occurring at the suction side of the blade) amount of erosion was measured. This erosion region is missing in the numerical results. An explanation for this would be that the inter-particle collisions are neglected in the numerical model. These collisions enhance the turbophoresis effect (the tendency of the particles to flow towards the low turbulence level) and with that, the particles flux towards the wall. The fact that the erosion increases while moving towards the trailing edge supports this explanation, since the turbophoresis effect would also yield a positive volume fraction gradient (and with that a positive erosion gradient) in the flow direction.

Conclusions

It is found that for the conditions that typically occur in a centrifugal dredge pump impeller, the Eulerian-Lagrangian method is appropriate for modelling the slurry flow.

The benchmark study with impinging jet showed that the fluid and particle velocities showed good correspondence with the experimental results. The largest deviation between the numerical model and the experiments could be found directly in line with the nozzle wall, which is due to the inability of the model to calculate the flow field at locations with large streamline curvature.

For the impeller model, it is found that the two-way coupled method provides significantly more accurate results than the one-way coupled method. A comparison between the different erosion models showed that the E/CRC erosion model overpredicts the erosion loss. In addition, the Finnie and Oka erosion models performed equally well for the validated region. However, due to the inability of the Finnie model to predict the erosion at and near the leading edge of the impeller blade, it can be concluded that the Oka model is the most suitable model for computing the erosion occurring in the centrifugal dredge pump impeller. A longer contact probe for the CMM machine would improve the validation of the numerical model since then the leading edge and suction part of the impeller could be measured and included in the analysis.

By comparing the numerical and experimental results (as calculated using the two-way coupled method), it is found that the erosion rate at the suction side of the blade is slightly underpredicted, while the results show good agreement qualitatively. For the pressure side of the blade, there are larger differences, although the major part of this side does not show any erosion at all for both the numerical and the experimental results.

Despite the modelling framework that contains many sub-models, limitations associated with the models are studied. The immediate takeaway from the study indicated the need to reduce the recirculation zone and smoothen the flow at the pressure side by correcting the flow incidence for the improvement in blade design. From the erosion study, it was found that more than 1 mm of material loss was seen in the suction side close to the trailing edge after the 55.7-hour experiment. This data is planned to be used for future research in the erosion analysis of the eroded geometry of the impeller. Future research to optimise the modelling framework for including for various working conditions, material, and sediment properties is expected to help set up a predictive maintenance plan for early detection of erosion problems.

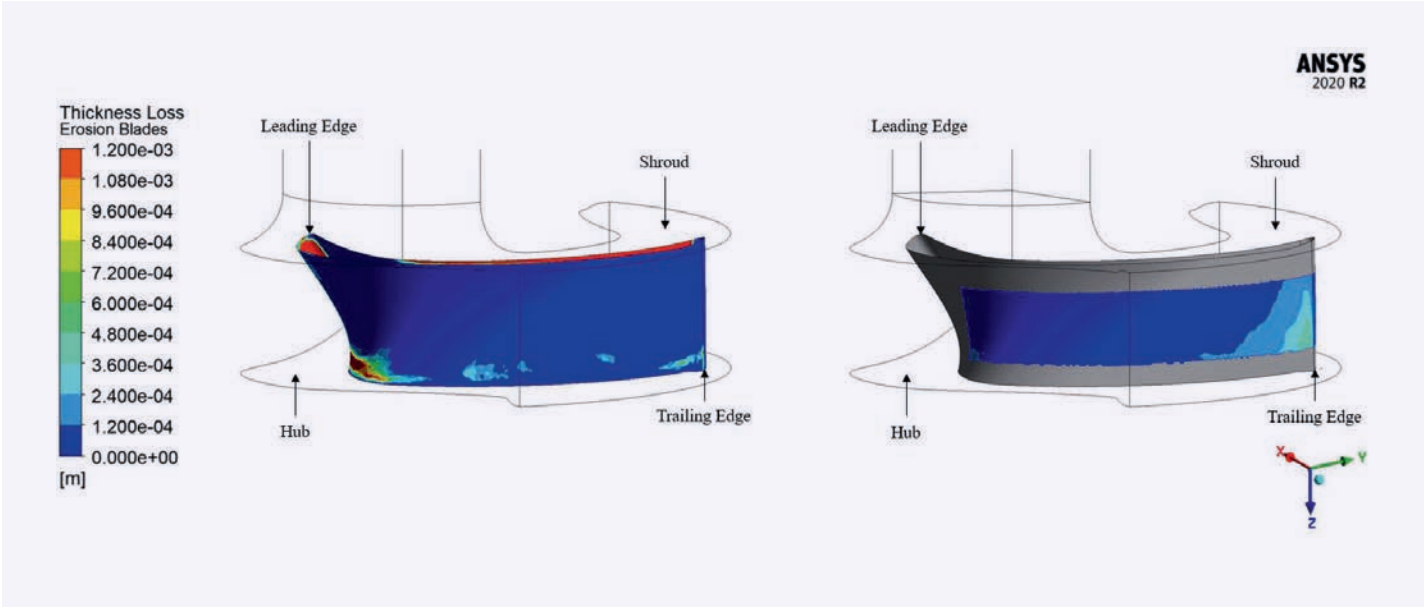

FIGURE 19

Erosion pattern on the pressure side of the blade for the two-way coupled numerical model (left) and the experiment (right).

René Kolman, IADC's Secretary General, presents the Young Author Award 2022 to Suman Sapkota for the co-authoring of his research paper, Estimating sediment erosion for centrifugal dredge pump's impeller. The award is presented at industry-leading conferences, with this year's winning author selected from the proceedings of WODCON XXIII, held in Copenhagen, Denmark, 16-20 May 2022.

Summary

The research is focused on validating and demonstrating a numerical model capable of estimating the erosion wear due to slurry flow on the impeller blades of a centrifugal dredge pump by using Computational Fluid Dynamics (CFD).

The numerical computations are performed using the commercial software ANSYS Fluent with the Eulerian–Lagrangian framework for the mixture of water and sand particles. For the turbulence of the water, the k-ω SST turbulence model is used. The collisions of the particles with the wall are modelled using the Grant–Tabakoff model, whereas the linear soft sphere model is used for the inter-particle collisions. Oka model is used for erosion modelling.

A benchmark study of submerged impinging jet and the numerical computation with impeller was performed as part of the numerical study and compared with the experimental results from the literature review. From the impinging jet benchmark, it is found that the fluid and particle velocity fields can be calculated with reasonable accuracy.

A numerical and experimental investigation has been conducted on the erosion of impeller blades close to the best efficiency conditions to predict the extent of the erosion wear concerning the velocity flow field, particle trajectories and other factors, such as particle diameter and grid size. Experiments were conducted in a facility that is available within the company Damen Dredging Equipment. For the quantification of the erosion wear, a Coordinate Measurement Machine (CMM) is used. By measuring several points on the impeller blade surface before and after a 55.7-hour experiment, the resulting erosion could be determined. The two-way coupled numerical model showed good correspondence with the experimental results.

Suman Sapkota

Trained as a mechanical engineer, Suman Sapkota works as a research, development and innovation engineer for Damen Dredging Equipment, in the Netherlands. He has a background in 3D modeling (CAD), computational fluid dynamics, finite element analysis and sustainable energy technology. Suman completed his MSc in sustainable energy technology (specialisation in engineering fluid dynamics) from the University of Twente, in the Netherlands. His specific research interests lie in fluid mechanics for turbomachines, cavitating flows, sediment erosion and fluid-structure interaction (FSI).

Wim Kleermaker

After gaining a BSc in Mechanical Engineering from HAN University of Applied Sciences, Wim Kleermaker obtained a master's degree in Aerospace Engineering at Delft University of Technology, in the Netherlands. He graduated on the subject of dredge pumps at the company Damen Dredging Equipment. In 2021, he joined the Maritime Research Institute Netherlands (MARIN) as a project engineer/specialist. Within this role, his focus is primarily on performing numerical simulations for offshore applications.

Ruud A.W.M. Henkes

In 1985, Ruud Henkes obtained an MSc (Hons) in Aerospace Engineering from Delft University of Technology (TU Delft), in the the Netherlands. He gained a PhD (Hons) in fluid flow and heat transfer in 1990 at the same university. Associate Professor Aerodynamics at TU Delft until 1997, he then joined the multiphase flow team of the Shell Technology Centre in Amsterdam. Ruud has held various roles as team lead and principal technical expert (Fluid Flow) at Shell. Since 2008, he has combined a (part-time) full professorship in multiphase flow at TU Delft and as of 2021 holds the position of Scientific Director of the J.M. Burgerscentrum for Fluid Mechanics.

Alexander van Zuijlen

Alexander is Assistant Professor at the aerodynamics section of the Faculty of Aerospace Engineering, Delft University of Technology (TU Delft), in the Netherlands. He obtained his doctorate in 2006 from TU Delft on the topic of computational fluid-structure interaction. Alexander's research focuses on development of numerical methods for multi-physics simulations and reduced order modeling for fluid-structure interaction applications.

References

Ahmad K., Baker R. C. and Goulas A. (1986)
Computation and experimental results of wear in a slurry pump impeller. *Journal of Mechanical Engineering Science*. 200(6): 439-445. doi. org/10.1243/PIME_PROC_1986_200_153_02

Andersson B., Andersson, R., Håkansson, L., Mortensen, M., Sudiyo, R., Wachem, B. Van. (2012)
Computational fluid dynamics for engineers. Cambridge University Press, Cambridge, UK.

ANSYS Inc. (2020a)
ANSYS Fluent theory guide. Canonsburg, PA, USA.

Celik I.B., Ghia U., Roache P.J., Freitas C.J., Coleman H. and Raad P.E. (2008)
Procedure for estimation and reporting of uncertainty due to discretization in CFD applications, *Journal of Fluids Engineering*, Vol. 130, no. 7.

Crowe C., Schwarzkopf J.D., Sommerfeld M. and Tsuji Y. (1998)
Multiphase flows with droplets and particles. CRC Press, Leiden, The Netherlands.

Finnie I. (1960)
Erosion of surfaces by solid particles. *Wear*, Volume 3, pp. 87-103.

Grant G. and Tabakoff W. (1975)
Erosion prediction in turbomachinery resulting from environmental solid particles. *Journal of Aircraft*, Volume 12, pp. 471-478.

Huang S., Huang J., Guo J. and Mo Y. (2019)
Study on wear properties of the flow parts in a centrifugal pump based on EDEM-Fluent coupling. *Processes*, p. 431.

Ilker P., and Sorgun M. (2020)
Performance of turbulence models for single phase and liquid-solid slurry flows in pressurized pipe systems. *Ocean Engineering*, Volume 214.

Keyence Corporation. (2021)
Coordinate measuring machines. Keyence Corporation, Osaka, Japan.

Krüger S., Martin N. and Dupont P. (2010)
Assessment of wear erosion in pump impellers. In proceedings of the 26th International Pump Users symposium. Winterhur, Switzerland.

Lai F., Zhu X., Xu X. and Li G. (2018).
Erosion wear and performance simulation of centrifugal pump for solid-liquid flow. In proceedings of the ASME 2018 POWER conference. Florida, USA.

Markus C. (2020)
Materiaaleigenschappen (Material properties). Bachelor's thesis. Damen Dredging Equipment, Nijkerk, The Netherlands.

Menter E.R. (1994)
Two-equation eddy-viscosity turbulence models for engineering applications. *AIAA Journal*, 832(8).

Miska S. J. (2008)
Particle and fluid velocity measurements for viscous liquids in a direct impingement flow resulting in material erosion. Master's thesis. University of Tusla, Tulsa, Oklahoma, USA.

Mitutoyo Corporation. (2021)
CRYSTA-APEX S. Mitutoyo, Kawasaki, Japan.

Nieuwstadt E.M., Boersma B.J. and Westerweel J. (2016)
Turbulence, Introduction to theory and applications of turbulent flows. Springer, Berlin, Germany.

Oka Y., Okamura K. and Yoshida T. (2005a)
Practical estimation of erosion damage caused by solid particle impact. Wear, 259 (Part 1: Effects of impact parameters on a predictive equation), pp. 95-101.

Oka Y., Okamura K. and Yoshida T. (2005b)
Practical estimation of erosion damage caused by solid particle impact. *Wear*, 259(Part 1: Mechanical properties of materials directly associated with erosion damage), pp. 102-109.

Roco M.C. and Addie G.R. (1987)
Erosion wear in slurry pumps and pipes. *Powder Technology*, 50(1), pp. 35-46.

Roco M.C., Addie G.R. and Visintainer R. (1985)
Study on casing performances in centrifugal slurry pumps. *Particulate Science and Technology*, Volume 3, pp. 65-88.

Sadighian A. (2016)
Investigating key parameters affecting slurry pipeline erosion. PhD thesis. University of Alberta, Edmonton, Alberta, Canada.

Sapkota S. (2018)
Technical and sustainability analysis of sediment erosion of impeller blades of dredge pumps. Master's thesis. University of Twente, Enschede, The Netherlands.

Tarodiya R. and Gandhi B.K. (2017)
Hydraulic performance and erosive wear of centrifugal slurry pumps – A review. *Powder Technology*, Issue 305, pp. 27-38.

Tarodiya R. and Gandhi B.K. (2019)
Experimental investigation of centrifugal slurry pump casing wear handling solid-liquid mixtures. *Wear*, pp. 434-435.

Wang Q., Huang Q., Sun X., Karmi S. and Shirazi S.A. (2021)
Experimental and numerical evaluation of the effect of particle size on slurry erosion prediction. *Journal of Energy Resources Technology*, Volume 143.

Wang Y., and Wang W.J. (2012)
Applicability of eddy viscosity turbulence models in low specific speed centrifugal pump. In proceeding of 26th IAHR symposium on Hydraulic Machinery and Systems, Volume 15.

Xiao Y., Guo B., Ahn S.H., Luo Y., Wang Z., Shi G. and Li Y. (2019)
Slurry flow and erosion prediction in a centrifugal pump after long-term operation. *Energies*, p.1523.

Zhang Y., Reuterfors E.P., McLaury B.S., Shirazi S.A. and Rybicki E.E. (2007)
Comparison of computed and measured particle velocities and erosion in water and air flows. *Wear*, Volume 263, pp. 330-338.

UPCOMING COURSES AND CONFERENCES

Dredging and Reclamation Seminar

7-11 November 2022
Grand Copthorne Waterfront Hotel (TBC)
Singapore

About the seminar

Since 1993, IADC has regularly held a week-long seminar developed especially for professionals in dredging-related industries. These intensive courses have been successfully presented in the Netherlands, Singapore, Dubai, Argentina, Abu Dhabi, Bahrain and Brazil. With these seminars, IADC reflects its commitment to education, encouraging young people to enter the field of dredging and improving knowledge about dredging throughout the world.

For whom

The seminar has been developed for both technical and non-technical professionals in dredging-related industries. From students and newcomers in the field of dredging to higher-lever consultants, advisors at port and harbour authorities, offshore companies and other organisations that carry out dredging projects. Attendees will gain a wealth of knowledge and a better understanding of the fascinating and vital dredging industry.

In the classroom

There is no other dredging seminar that includes a workshop covering a complete tendering process from start to finish. The in-depth lectures are presented by experienced dredging professionals from IADC member companies. Their practical knowledge and professional expertise are invaluable for in the classroom-based lessons. Among the subjects covered are:

- the development of new ports and maintenance of existing ports;
- project development: from preparation to realisation;
- descriptions of types of dredging equipment;
- costing of projects;
- types of dredging projects; and
- environmental aspects of dredging.

COVID-19

Due to the COVID-19 pandemic, events can be postponed or cancelled. IADC has been following the Dutch authorities' advisory measures with regard to limiting the spread of the virus and is keeping a close eye on the situation. We advise checking the IATA website regularly for COVID-19 travel regulations per country (https://www.iatatravelcentre.com).

The seminar has been developed for both technical and non-technical professionals in dredging-related industries.

Site visit

Practical experience is priceless and is what sets this seminar apart from all others. A site visit to a dredging yard or project is therefore part of the programme and allows participants to view and experience dredging equipment firsthand to gain better insights into the multifaceted field of dredging operations.

Networking

Networking is invaluable. A mid-week dinner where participants, lecturers and other dredging employees can interact, network, and discuss the real, handson world of dredging provides another dimension to this stimulating week.

Certificate of achievement

Each participant will receive a set of comprehensive proceedings and at the end of the week, a certificate of achievement in recognition of the completion of the coursework. Full attendance is required to attain the certificate.

Costs

The fee for the week-long seminar is EUR 3,100 (out of scope EU VAT). The fee includes all tuition, proceedings, workshops and a special participants' dinner, but excludes travel costs and accommodation. For more information and how to register visit https://bit.ly/IADC-events.

PIANC's Early Contractor Involvement Conference

6 October 2022
Hendrik Conscience Building
Brussels, Belgium

PIANC, in cooperation with IADC, presents a 1-day conference on Early Contractor Involvement (ECI). How can early involvement of the main contractor and its supply chain create value for the developer of an infrastructure project? And how should such an early collaboration be structured from a procurement, contractual and organisational perspective? These are the overarching questions that will be explored during the conference.

PIANC has formed the Working Group 94; "A framework for Early Contractor Involvement (ECI) in infrastructure projects" with ECI experts and practitioners to develop a report containing practical guidance how to perform ECI projects. This full-day conference will address the topics of the report, with speakers from the working group and other leading experts in ECI and collaborative contracting. For more information and how to register visit https://bit.ly/ECI61022.

Conference Knowledge and Innovation Programme

Marker Wadden (KIMA)
12-14 October 2022
Amsterdam, The Netherlands

An example of Building with Nature, Marker Wadden is an archipelago of nature islands created with excess sediment from Lake Markermeer. Over the past 5 years, the islands have been extensively researched on the themes of building with fine sediment, ecosystem development and governance. The congress invites professionals involved in ecological restoration and management of shallow lakes, related to climate adaptation and biodiversity, to come and learn about the research results and to visit the islands. To register, visit https://bit.ly/MWadden.

Dredging for Sustainable Infrastructure Course

13-14 December 2022
HR Wallingford Oxfordshire, UK

For professionals involved in dredging related activities for water infrastructure development, CEDA and IADC present the Dredging for Sustainable Infrastructure course. How to achieve dredging projects that fulfil primary functional requirements, while adding value to the natural and socio-economic systems. This is just one of the questions addressed during the 2-day course that is based on the philosophy of the book, *Dredging for Sustainable Infrastructure*.

This course, like the book, fills a gap: it gives guidance to professionals on how to bring into practice the new thinking that in many ways has transformed dredging in the last decade. Therefore, the course is essential for professionals driven by the ambition to achieve sustainable and resilient water infrastructure with a dredging that component that contribute to the UN's Sustainable Development Goals.

Experienced lecturers will describe the latest thinking and approaches, explain methodologies and techniques, and demonstrate through engaging workshops and case studies, how to implement the sustainability principles into dredging project practice. Register for the course at https://bit.ly/DfSIcourseUK

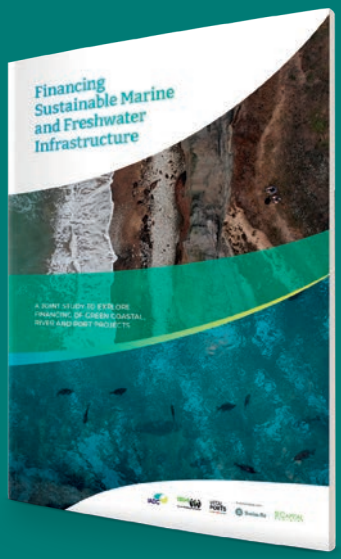

Financing Sustainable Marine and Freshwater Infrastructure Conference

February 2023 (date to be confirmed)
Mövenpick Jumeirah Beach Hotel
Dubia, UAE

How can private capital accelerate the green transition in marine and freshwater infrastructure? This is the overarching question that will be explored during the IADC conference, Financing Sustainable Marine and Freshwater Infrastructure. The 1-day conference aims to create awareness for the need to clarify sustainable concepts and associated financial structures in order to familiarise the financial sector with the financing of green coastal, river and port projects, and to develop ideas to bring this to mainstream infrastructure investment asset classes. The report, *Financing Sustainable Marine and Freshwater Infrastructure: A joint study to explore financing of green coastal, river and port projects*, will provide the basis of the conference programme. For more information and how to register visit https://bit.ly/ConfDubai2022.

Main members

DEME Group
Head office Belgium
+32 3 250 5211
info@deme-group.com
www.deme-group.com

Dutch Dredging
Head office The Netherlands
+31 184 411 999
info@dutchdredging.nl
www.dutchdredging.nl/en

Group De Cloedt – DC Industrial N.V.
Head office Belgium
+32 2 647 12 34
office@groupdecloedt.be
www.groupdecloedt.be

Gulf Cobla (L.L.C.)
Head office United Arab Emirates
+971 4 803 7777
gc-info@gulfcobla.com
www.gulfcobla.com

Hyundai Engineering & Construction Co., Ltd.
Head office South Korea
+82 2 746 1114
webmaster@hdec.co.kr
www.hdec.co.kr

Jan De Nul Group
Head office Luxembourg
+352 39 89 11
info@jandenulgroup.com
www.jandenul.com

National Marine Dredging Company
Head office United Arab Emirates
+971 2 5130000
nmdc@nmdc.ae
www.nmdc.com

Penta-Ocean
Head office Japan
+81 3 3817 7181
poc_international_web@mail.penta-ocean.co.jp
www.penta-ocean.co.jp

Rohde Nielsen A/S
Head office Denmark
+45 33 91 25 07
mail@rohde-nielsen.dk
www.rohde-nielsen.dk

Royal Boskalis Westminster N.V.
Head office The Netherlands
+31 78 6969 000
royal@boskalis.com
www.boskalis.com

TOA Corporation
Head office Japan
+81 3 6757 3800
webmaster@toa-const.co.jp
www.toa-const.co.jp

Van Oord
Head office The Netherlands
+31 88 8260 000
info@vanoord.com
www.vanoord.com

Colophon

Correction: Photo credit for the front cover Winter 2021 issue was incorrectly stated as Boskalis and should be credited to John Gundlach.

Editorial
For editorial enquiries, please email editor@iadc-dredging.com or call +31 (0)70 352 3334. Articles featured in *Terra et Aqua* do not necessarily reflect the opinion of the IADC Board of Directors or of individual members.

Editor
Ms Sarah Nunn

Editorial Advisory Committee
Mr Robert de Bruin, Chair
Mr René Kolman, Secretary General
Mrs Vicky Cosemans
Mrs Heleen Schellinck
Mr Arno Schikker

Board of Directors
Mr Frank Verhoeven, President
Mr Junji Katsumura, Vice President
Mrs Els Verbraecken, Treasurer
Mr Theo Baartmans
Mr Niels de Bruijn
Ms Mieke Fordeyn
Mr Neil Haworth
Mr Philip Hermans

Front cover
Photo © Jan De Nul Group

Back cover
Photo © Jan De Nul Group

Design
Smidswater, The Hague, The Netherlands

Layout
Robert Dumay Graphic Design, Zierikee, The Netherlands

Printing
Tuijtel B.V., Hardinxveld-Giessendam, The Netherlands

ISSN 0376-6411

How to subscribe?
To receive a free print or digital subscription, register at www.iadc-dredging.com/terra-et-aqua/subscribe.

Call for submissions
Published quarterly, *Terra et Aqua* is an educational and professional resource that features cutting-edge innovations to disseminate knowledge throughout the dredging industry. Are you an author, researcher or expert in dredging or a related field? Do you want to share your innovative research, papers or publications with the dredging industry? Then submit your proposals to the editor at editor@iadc-dredging.com for consideration.

Terra et Aqua is published four times a year by
International Association of Dredging Companies
Stationsplein 4
2275 AZ Voorburg
The Netherlands
www.iadc-dredging.com